PCP
PLANT & CELL PHYSIOLOGY

The Mitochondrial Thioredoxin System Contributes to the Metabolic Responses Under Drought Episodes in Arabidopsis

Paula da Fonseca-Pereira[1,2], Danilo M. Daloso[1,5], Jorge Gago[1,3], Franklin Magnum de Oliveira Silva[2], Jorge A. Condori-Apfata[2], Igor Florez-Sarasa[1], Takayuki Tohge[1], Jean-Philippe Reichheld[4], Adriano Nunes-Nesi[2], Alisdair R. Fernie[1] and Wagner L. Araújo[2,*]

[1]Max-Planck-Institut für Molekulare Pflanzenphysiologie, Am Mühlenberg 1, D-14476 Potsdam-Golm, Germany
[2]Max-Planck Partner Group, Departamento de Biologia Vegetal, Universidade Federal de Viçosa, 36570-900 Viçosa, Minas Gerais, Brazil
[3]Research Group on Plant Biology under Mediterranean Conditions, Universitat de les Illes Balears, 07122 Palma de Mallorca, Illes Balears, Spain
[4]Laboratoire Génome et Développement des Plantes, Unité Mixte de Recherche 5096, Centre National de la Recherche Scientifique, Université de Perpignan Via Domitia, 66860 Perpignan, France
[5]Present address: Departamento de Bioquímica e Biologia Molecular, Universidade Federal do Ceará, Fortaleza, Ceará, Brasil.
*Corresponding author: E-mail, wlaraujo@ufv.br; Fax, +55 31 3899 2580.
Subject areas: (2) environmental and stress responses, and (5) photosynthesis, respiration and bioenergetics.
(Received May 24, 2018; Revised September 24, 2018)

Thioredoxins (Trxs) modulate metabolic responses during stress conditions; however, the mechanisms governing the responses of plants subjected to multiple drought events and the role of Trxs under these conditions are not well understood. Here we explored the significance of the mitochondrial Trx system in Arabidopsis following exposure to single and repeated drought events. We analyzed the previously characterized NADPH-dependent Trx reductase A and B double mutant (*ntra ntrb*) and two independent mitochondrial thioredoxin o1 (*trxo1*) mutant lines. Following similar reductions in relative water content (~50%), Trx mutants subjected to two drought cycles displayed a significantly higher maximum quantum efficiency (F_v/F_m) and were less sensitive to drought than their wild-type counterparts and than all genotypes subjected to a single drought event. Trx mutant plants displayed a faster recovery after two cycles of drought, as observed by the higher accumulation of secondary metabolites and higher stomatal conductance. Our results indicate that plants exposed to multiple drought cycles are able to modulate their subsequent metabolic and physiological response, suggesting the occurrence of an exquisite acclimation in stressed Arabidopsis plants. Moreover, this differential acclimation involves the participation of a set of metabolic changes as well as redox poise alteration following stress recovery.

Keywords: *Arabidopsis thaliana* • Metabolic acclimation • Mitochondrial Trx system • Respiration • Tricarboxylic acid cycle • Water limitation.

Abbreviations: Col-0, Columbia ecotype; DAHP, 3-deoxy-d-*arabinoheptulosonate* 7-phosphate; DRIP2, DREB2A-INTERACTING PROTEIN2; *ETR*, electron transport rate; F_m, maximum chlorophyll fluorescence; F_s, steady-state fluorescence; F_v, variable chlorophyll fluorescence; GC-MS, gas chromatography coupled with mass spectrometry; g_m, mesophyll conductance; LC-MS, liquid chromatography coupled with mass spectrometry; NTR, NADPH-dependent Trx reductase; NTS, NADPH-dependent thioredoxin system; PARi, incident photosynthetically active radiation; PCA, principal component analysis; φPSII, photochemical efficiency of photosystem II; RD 29A, drought responsive A; RD 29B, drought responsive B; RT-PCR, real time PCR; RWC, relative water content; trxo1, thioredoxin o1; TCA, tricarboxylic acid; TW, turgid weight; WT, wild type.

Introduction

Limited water availability is the most common environmental stress affecting plant growth and production (Walter et al. 2011). Indeed, it is expected that drought events will become more widespread and severe due to climate changes, affecting plant performance and crop yield (Walter et al. 2011, Anjum et al. 2016, Swann et al. 2016). Hence, a better understanding of how plants respond and acclimate to drought episodes via suitable physiological and molecular responses is a fundamental step in the development of stress-tolerant crops (Cattivelli et al. 2008, Ding et al. 2013). Therefore, a considerable number of studies have focused on seeking differential responses of plants pre-exposed to dehydration stress treatments in contrast to plants that were not previously stressed (Ding et al. 2012, Ding et al. 2013, Ding et al. 2014, Virlouvet et al. 2014, Virlouvet and Fromm 2015, Crisp et al. 2016).

It is well established that cell redox homeostasis is disturbed under dehydration stress (Noctor et al. 2014). In addition, one of the important factors determining the effect of water deficit on plant productivity is its impact on mitochondrial respiration (Zivcak et al. 2016). Thus, it is expected that mitochondrial redox proteins can exert a prominent role in drought responses. Accordingly, some of the most important thiol-based enzymes involved in cellular redox homeostasis management are the thioredoxins (Trxs) (König et al. 2012). Trxs are widely distributed regulatory proteins with two reactive cysteines that confer reductive properties and allow the precise regulation of specific

Plant Cell Physiol. 60(1): 213–229 (2019) doi:10.1093/pcp/pcy194, Advance Access publication on 17 October 2018, available online at www.pcp.oxfordjournals.org

target proteins (Lázaro et al. 2013). In plants, they were identified some time ago as mediators between light-driven electron transport and dark carbohydrate metabolism in chloroplasts (Buchanan 1980, Mock and Dietz 2016). In plant mitochondria, and other cellular compartments, a growing body of information concerning Trx redox regulation has been obtained via the application of proteomics and mass spectrometry-based techniques (Laloi et al. 2001, Balmer et al. 2004, Reichheld et al. 2005, Reichheld et al. 2007, Yoshida et al. 2013, Schmidtmann et al. 2014, Daloso et al. 2015, Møller 2015). Currently, a functional NADPH-dependent Trx system (NTS) in plants is known to be localized in both the cytosol and mitochondria and to be comprised of two highly similar isoforms of NADPH-dependent Trx reductase (NTR), A and B, that are encoded by two distinct genes in Arabidopsis (Laloi et al. 2001, Reichheld et al. 2005). In addition, the extraplastidial NTS is composed of both the subfamily Trx *h*, which is present in the cytosol, nucleus, mitochondria and the plasma membrane, and the subfamily Trx *o* present in mitochondria and the nucleus (Geigenberger et al. 2017). Both subfamilies are, in turn, reduced by NTRA or NTRB.

More than 100 mitochondrial Trx target candidate proteins have been identified by mutant Trx affinity columns in conjunction with proteomics (Balmer et al. 2004, Yoshida et al. 2013). The putative targets are involved in a broad range of mitochondrial processes including photorespiration, ATP synthesis and stress-related reactions. Moreover, tricarboxylic acid (TCA) cycle enzymes and associated pathways were both confirmed as Trx targets *in vitro* and *in vivo* (Schmidtmann et al. 2014, Yoshida and Hisabori 2014, Daloso et al. 2015). Taken together, these results suggest that mitochondria, similarly to plastids, use Trx and redox status to regulate their main carbon flux pathway (Daloso et al. 2015). In general, TCA cycle enzymes are additionally highly susceptible to oxidative stress (Winger et al. 2007, Obata et al. 2011), which probably involves the participation of the Trx system by mechanisms that are as yet not fully understood. Collectively, this information suggests an important, albeit somewhat neglected, manner by which mitochondrial metabolism is regulated in response to various stresses in plants.

To date, three functional NTRs have been found in Arabidopsis, including the plastidial NTRC, for which a large number of studies have described its association with plant protection against oxidative stress (Serrato et al. 2004, Spínola et al. 2008, Chae et al. 2013, Lepistö et al. 2013, Correa-Aragunde et al. 2015, Moon et al. 2015, Naranjo et al. 2016). In contrast, the potential significance of NTRA and NTRB under stress conditions remains poorly explored probably due to the functional redundancy between the cytosolic and mitochondrial forms (Geigenberger et al. 2017). This fact apart, it was demonstrated that NTRA-overexpressing plants have a higher stress tolerance against oxidative and drought stresses via the regulation of levels of reactive oxygen species (ROS) (Cha et al. 2014, Cha et al. 2015). In addition, in contrast to *ntra* and *ntrb* single knockout mutants, which show no visible phenotypic modifications under normal conditions, the double *ntra ntrb* mutant exhibited major differences. The *ntra ntrb* plants were characterized as producing wrinkled seeds, exhibiting slow rates of plant growth and accumulating high levels of anthocyanins (Reichheld et al. 2007, Bashandy et al. 2009), which could be expected to increase tolerance to abiotic stresses such as drought (Sperdouli and Moustakas 2012, Kovinich et al. 2014). Furthermore, a role for Trx *o1* in redox homeostasis during seed germination under salt conditions was recently demonstrated (Ortiz-Espín et al. 2017).

Here we have attempted to characterize the functional role of the mitochondrial Trx system following exposure to drought, and further investigate whether the re-exposure to a drought event would cause more rapid or stronger metabolic and physiological adjustments. To this end, we evaluated the differential acclimation mechanisms associated with drought tolerance in mutants of the mitochondrial Trx pathway, namely the NADPH-Trx reductase *a* and *b* double mutant (*ntra ntrb*) and the mitochondrially located thioredoxin *o1* (*trxo1*) mutant. Our results demonstrate that the absence of a functional mitochondrial Trx system leads to an enhanced drought tolerance and that following multiple events of drought the Trx system seems to be of key importance.

Results

Mitochondrial Trx mutants under water deficit conditions

To investigate the functional role of the mitochondrial Trx pathway during water shortage, we analyzed the previously characterized *NADP-TRX* reductase *a* and *b* double knockout mutant (*ntra ntrb*) plant that does not express two NTR isoforms localized in the cytosol and mitochondria (Reichheld et al. 2007). In addition, we isolated two independent lines that contained T-DNA elements inserted into the Trx o1 (*trxo1*) gene (At2g35010) encoding a mitochondrial Trx from the Salk collection (SALK 042792 and SALK 143294) and confirm that transcripts of *TRXo1* are absent in these mutant lines (Supplementary Fig. S1).

Following the characterization of the molecular identity of the T-DNA insertional mutants, they were grown alongside wild-type (WT) control plants. There were no visible aberrant phenotypes in the mutants during vegetative growth under normal watering conditions (Fig. 1A, left panel). In a first experiment, plants cultivated in single pots were exposed to drought stress (**Fig. 1**). At 10 d after the suspension of irrigation, all the genotypes presented early symptoms of chlorosis and leaf wilting, yet the WT exhibited more severe dehydration symptoms than the mutants (**Fig. 1A**, middle panel). To investigate further the development of drought stress symptoms, we next analyzed the relative water content (RWC) and the F_v/F_m (**Fig. 1B and C**, respectively). During the extended period of water withholding, all genotypes studied showed similar RWC values at all the time points evaluated here (**Fig. 1B**). After 10 d without watering, an important reduction in the RWC was observed for all genotypes, with a water loss of approximately 40% of the initial RWC (**Fig. 1B**). Moreover, reductions in F_v/F_m values were observed in all genotypes following the cessation of irrigation (**Fig. 1C**). To assess the capacity of the plants to recover following 10 d of water restriction, irrigation was restored. All genotypes investigated were able to rescue their original RWC

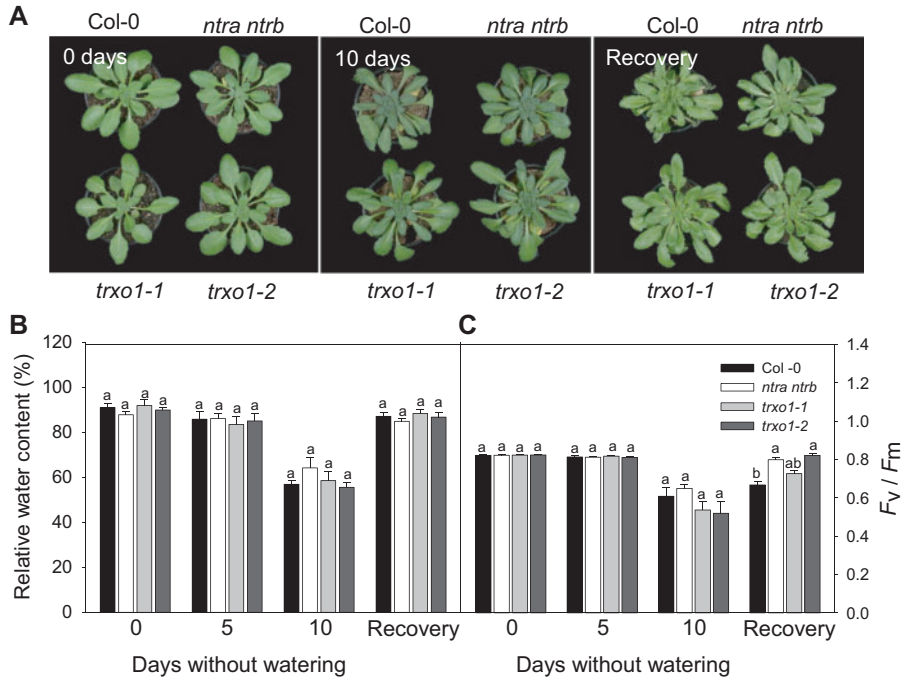

Fig. 1 Phenotype of Trx Arabidopsis mutants and wild-type plants (WT) under drought stress treatment. (A) Images of 4-week-old, short-day-grown Arabidopsis plants immediately (0 d) and after further treatment for 10 d without watering and on recovery irrigation for 3 d. (B) Relative water content (RWC) and (C) the maximum quantum yield of PSII electron transport (F_v/F_m) of leaves of 4-week-old, short-day Arabidopsis plants after further treatment for 0, 5 and 10 d without watering and on recovery. Values are means ± SE of five independent samplings. Different letters represent values that were judged to be statistically different between treatments by Tukey's multiples comparison's test ($P < 0.05$).

(i.e. at day 0, under non-stress conditions) after rehydration (**Fig. 1B**). On the other hand, only the mutant lines *ntra ntrb* and *trxo1-2* showed F_v/F_m values after recovery similar to those observed before the water deficit period (**Fig. 1C**), indicating that the water availability was enough to recover fully the photosynthetic capacity of these plants. Importantly, WT plants were not able to recover the F_v/F_m values following the restoration of irrigation, suggesting that the Trx mutants were less sensitive to drought stress.

Metabolic changes of Arabidopsis Trx mutants under water deficit conditions

In order to obtain a more detailed characterization of the functional significance of the mitochondrial Trx system under water deprivation, we next measured the levels of a broad range of primary (**Fig. 2**; Supplementary Data set I) and secondary (**Fig. 3**; Supplementary Data set II) metabolites in the plants during water deficit treatment. It should be noted that the levels of only relatively few metabolites were significantly different in the mutants in comparison with the WT at 0 and 5 d following the onset of drought (**Fig. 2**; Supplementary Data set I). Gas chromatography coupled with mass spectrometry (GC-MS) data revealed that, of the alterations observed under non-stress conditions, all the metabolites that changed significantly in the mutants were lower than the values observed in WT plants, including the decrease in valine in all mutants and in both serine and lysine in *trxo1-2* mutants. Conversely, as early as 5 d of water deficit, the majority of amino acids increased significantly only in *trxo1-1* plants in relation to WT values. Notably, the majority of the differences in primary metabolite levels was observed under more advanced stress (10 d) and on recovery. Following 10 d without watering, *trxo1-2* mutants showed higher levels of amino acids (alanine, ß-alanine, isoleucine, glutamate, lysine, methionine, ornithine, phenylalanine, serine, threonine, tyrosine, valine and tryptophan), organic acids [ascorbate, fumarate, γ-aminobutyric acid (GABA), glycolate and threonate] and other metabolites such as putrescine and hydroxyproline, when compared with WT plants. In addition, all mutant genotypes showed increased levels of trehalose and raffinose, metabolites that usually accumulate in tolerant plants subjected to desiccation (Valliyodan and Nguyen 2006, Obata and Fernie 2012, Arbona et al. 2013). Accordingly, after 10 d of drought, significant changes in a number of secondary metabolites for the mutant lines *trxo1-1* and *trxo1-2* were observed, including decreases in flavonol glycosides (K3G7R and K3R7R), and in the aliphatic glucosinolate 7MTH, in addition to the lower levels of anthocyanin and in the hydroxycinnamates sinapoyl-glucoside (SinG) and di-sinapoyl-glucoside (di-SinG) detected in the three mutants compared with WT plants (**Fig. 3**; Supplementary Data set II). The levels of only one secondary metabolite (7MTH) were significant altered in the *trxo1-1* mutants, while no differences were observed for the other mutants following recovery. On the other hand, a large number of changes in primary metabolites were evident following re-irrigation in the *ntra ntrb* double knockout plants and

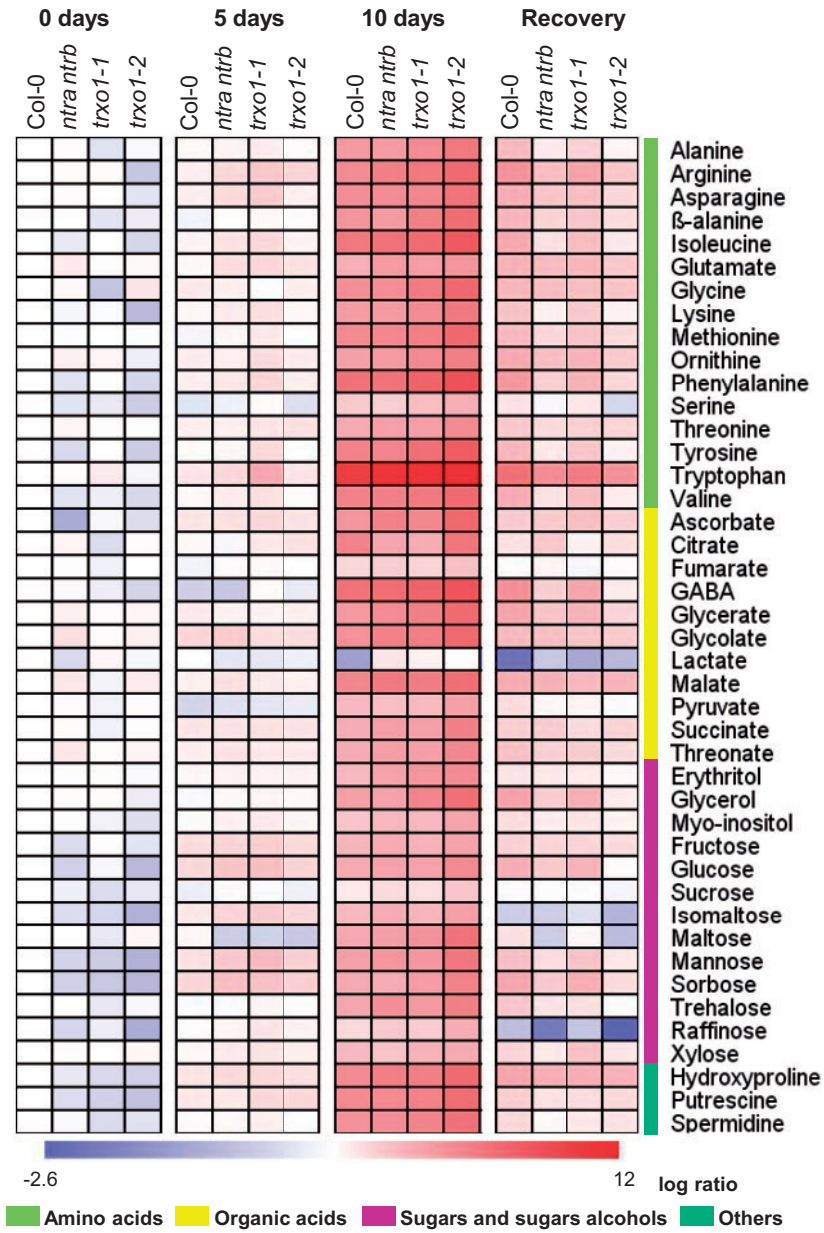

Fig. 2 Heat map representing the changes in relative abundance of metabolite levels as measured by GC-MS in Arabidopsis knockout mutants *ntra ntrb*, *trxo1-1* and *trxo1-2*, and wild type plants (WT) after further treatment for 0, 5 and 10 d without watering and on recovery irrigation for 3 d. Relative $\log_2$-transformed values of signal intensities were normalized with respect to the mean response calculated for the wild type control at day 0. Values are means ± SE of five independent samplings.

trxo1-2 plants, whereas only six metabolites (alanine, arginine, phenylalanine, tyrosine, pyruvate and putrescine) were significantly different in *trxo1-1* plants compared with the WT. Note that there was a general increase in the levels of primary metabolites in all genotypes both following drought (10 d) and on recovery in comparison with the initial condition (0 day). In contrast to the situation observed following 10 d of drought, there is a clear pattern of down-regulation of the majority of the primary metabolites in the mutants following the recovery, compared with WT levels (**Fig. 2**; Supplementary Data set I). For example, the *trxo1-2* and *ntra ntrb* plants displayed lower levels of several amino acids, including aromatic amino acids (phenylalanine, tyrosine and tryptophan) and two branched-chain amino acids (BCAAs), isoleucine and valine, as compared with WT levels. Moreover, the levels of organic acids (GABA, glycerate, pyruvate and threonate), sugars (fructose, mannose, maltose and sorbose) and sugar alcohols, such as glycerol and *myo*-inositol, were also lower than in WT plants in both *trxo1-2* and *ntra ntrb* mutants on recovery. Double mutant and *trxo1-2* plants were also characterized by lower levels of hydroxyproline and putrescine, while only *ntra ntrb* mutants displayed reductions in spermidine, in comparison with the WT on recovery.

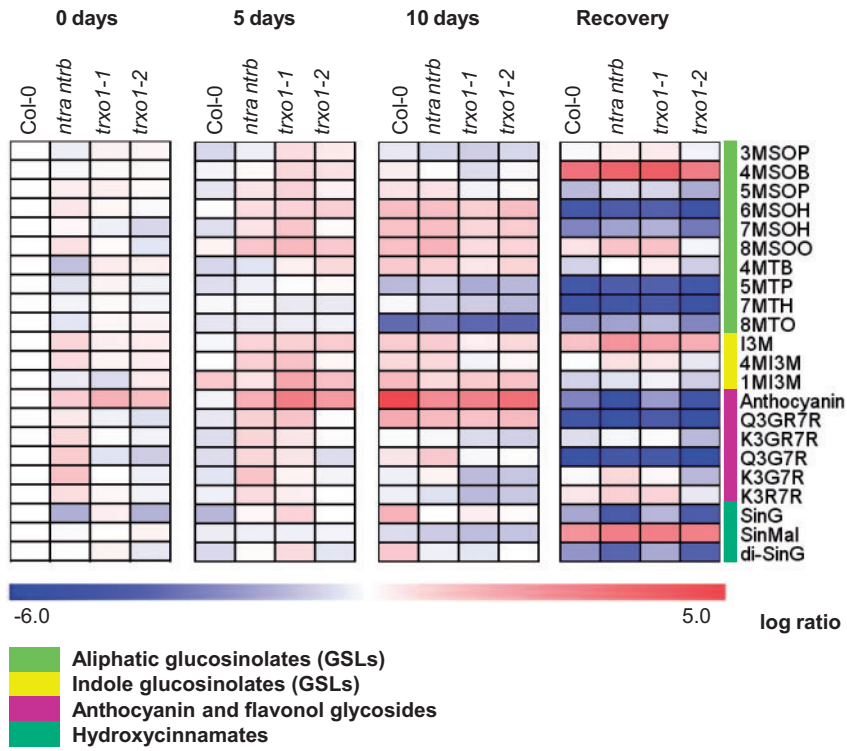

Fig. 3 Heat map representing the changes in relative abundance of secondary metabolite levels as measured by LC-MS in Arabidopsis knockout mutants *ntra ntrb*, *trxo1-1* and *trxo1-2*, and wild type plants (WT) after further treatment for 0, 5 and 10 d without watering and on recovery irrigation for 3 d. Relative $\log_2$-transformed values of signal intensities were normalized with respect to the mean response calculated for the WT control at day 0. Values are means ± SE of five independent samplings. Glucosinolates: 3MSOP, 3-methylsulfinylpropyl glucosinolate; 4MSOB, 4-methylsulfinylbutyl glucosinolate; 5MSOP, 5-methylsulfinylpentyl glucosinolate; 6MSOH, 6-methylsulfinylhexyl glucosinolate; 7MSOH, 7-methylsulfinylheptyl glucosinolate; 8MSOO, 8-methylsulfinyloctyl glucosinolate; 4MTB, 4-methylthiobutyl glucosinolate; 5MTP, 5-methylthiopentyl glucosinolate; 7MTH, 7-methylthioheptyl glucosinolate; 8MTO, 8-methylthiooctyl glucosinolate; I3M, indolyl-3-methyl glucosinolate; 4MI3M, 4-methoxy-indol-3-ylmethyl-glucosinolate; 1MI3M, 1-methoxy-3-indolylmethyl glucosinolate. Anthocyanin and flavonol glycosides: A11, anthocynin; Q3GR7R, quercetin-3-*O*-(2″-*O*-rhamnosyl)glucoside-7-*O*-rhamnoside; K3GR7R, kaempferol-3-*O*-(2″-*O*-rhamnosyl)glucoside-7-O-rhamnoside; Q3G7R, quercetin-3-*O*-glucoside-7-*O*-rhamnoside; K3G7R, kaempferol-3-*O*-glucoside-7-*O*-rhamnoside; K3R7R, keampferol-3-*O*-rhamnoside-7-*O*-rhamnoside. Hydroxycinnamates and aromatic amino acid: SinG, sinapoyl-glucoside; SinMal, sinapoyl-malate; di-SinG, di-sinapoyl-glucoside.

Differential response of Trx mutant plants submitted to single and recurrent drought events

Given the wide range of metabolic changes previously observed in Trx mutant plants exposed to a single drought episode, we next decided to evaluate the responses of plants submitted to a recurrent dehydration stress (**Fig. 4**). To this end, we performed another experiment with large pots with plants growing side by side and where there was one plant representing each genotype per pot (**Fig. 4A**). By doing this, we could ensure comparison of the responses in similar soil conditions and could be confident that the water restriction was highly similar across all genotypes.

All genotypes showed similar RWC values under any given condition (**Fig. 4B**). The RWC was similarly reduced in plants following one (D1) or two (D2) drought events, and none of the genotypes was able to recover the RWC fully after re-irrigation (**Fig. 4B**). F_v/F_m values (**Fig. 4C**) were only slightly lower in plants exposed to one (D1) or two (D2) drought events, in comparison with their respective controls (DC). Mutant plants previously exposed to a water suspension event (D2) displayed higher F_v/F_m values than the WT following the same treatment.

Trx-mediated redox regulation seems to be important for stomatal behavior during drought recovery

We further investigated whether gas exchange and Chl *a* fluorescence parameters might be affected in the mutant plants (Supplementary Table S2; Supplementary Fig. S3). No differences were observed for any of these parameters in any of the Trx mutants under optimal growth conditions. We next decided to evaluate if the exposure to drought followed by a recovery event could influence these photosynthetic parameters. For this purpose, we analyzed only the photosynthetic responses of re-watered plants (R2) (Supplementary Table S2), since it was virtually impossible to analyze precisely plants from D1, D2 and R1 due to their very low gas exchange rates (ΔCO_2 <0.5 in a flow of 100 μmol mol^{-1} air; data not shown). Interestingly, g_s was higher in the mutant lines at R2 compared with their WT counterparts (Supplementary Table S2; Supplementary Fig. S3). This indicates that, for the same water losses (**Fig. 4B**), Trx mutant lines are able to maintain their photosynthetic apparatus close to a normal functionality. In addition, *trxo1-2* plants showed a

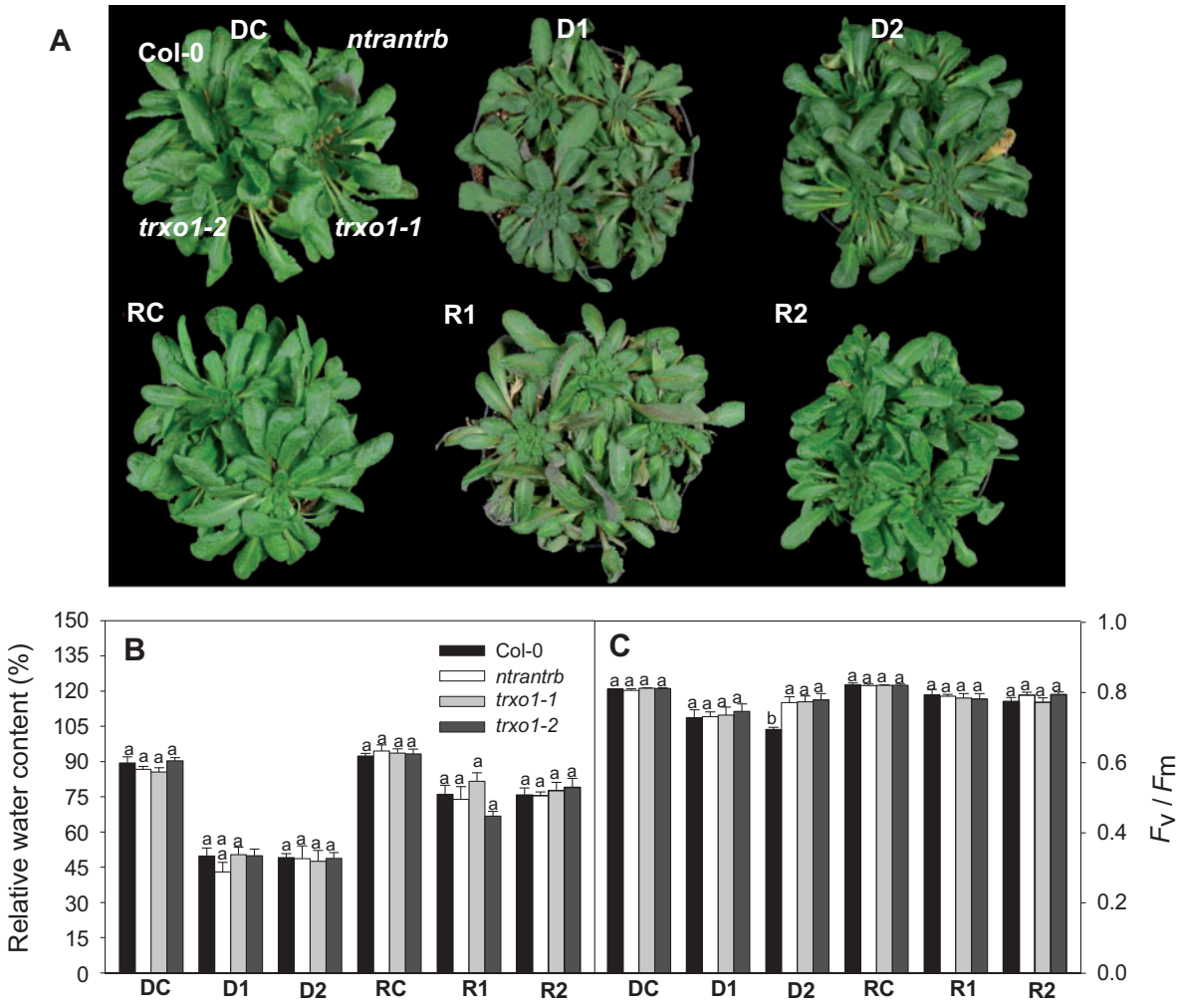

Fig. 4 Phenotype of Trx Arabidopsis knockout mutants and wild-type plants (WT) during dehydration and following rehydration. (A) Images of short-day-grown Arabidopsis plants immediately (DC and RC) and after further treatment for 10 d without watering (D1 and D2) and on recovery irrigation (R1 and R2) for 3 d. (B) Relative water content (RWC) and (C) the maximum quantum yield of PSII electron transport (F_v/F_m) of leaves of short-day-grown Arabidopsis plants. The data represents six conditions: unstressed control (DC), plants drought stressed only once (D1) and twice (D2), unstressed recovery control (RC) and rehydration of plants previously drought stressed once (R1) or twice (R2). Data represent averages of six biological replicates per genotype and condition. Different letters represent values that that were judged to be statistically different between treatments by Tukey's multiple comparison test ($P < 0.05$).

higher chloroplastic CO_2 concentration (C_c). Thus, when taken together, these results indicate a better recovery of g_s in Trx mutant plants following drought conditions.

Differential metabolic responses of Arabidopsis Trx mutants submitted to a repeated drought event compared with plants not previously stressed

We next evaluated the effect of a consecutive stress event on the metabolic response of the plants by measuring the levels of starch, sugars and nitrate at the middle of the day in illuminated leaves of mutants and the WT, as well as a broad range of primary and secondary metabolites. Drought decreased the levels of starch (Supplementary Fig. S4) coupled with increases in the levels of sucrose (Supplementary Fig. S4), glucose (Supplementary Fig. S4) and nitrate in all genotypes analyzed (Supplementary Fig. S5). We also observed a significant decrease in starch (RC) coupled with lower levels of sucrose (R1) and glucose (D2) in the *ntra ntrb* mutant compared with the WT under the same condition.

By using GC-MS-based metabolite profiling, we further observed a remarkable metabolic adjustment in response to the drought treatments (**Fig. 5**; Supplementary Data set III). Overall, the levels of most amino acids and organic acids increased significantly in plants that were subjected to drought stress either once (D1) or twice (D2) and even following re-irrigation (R1 and R2). Compared with WT plants, *ntra ntrb* plants exposed to one single drought event (D1) were characterized by several changes in amino acid levels, including a higher accumulation of asparagine, ornithine and the aromatic amino acids phenylalanine and tryptophan. In addition, we also

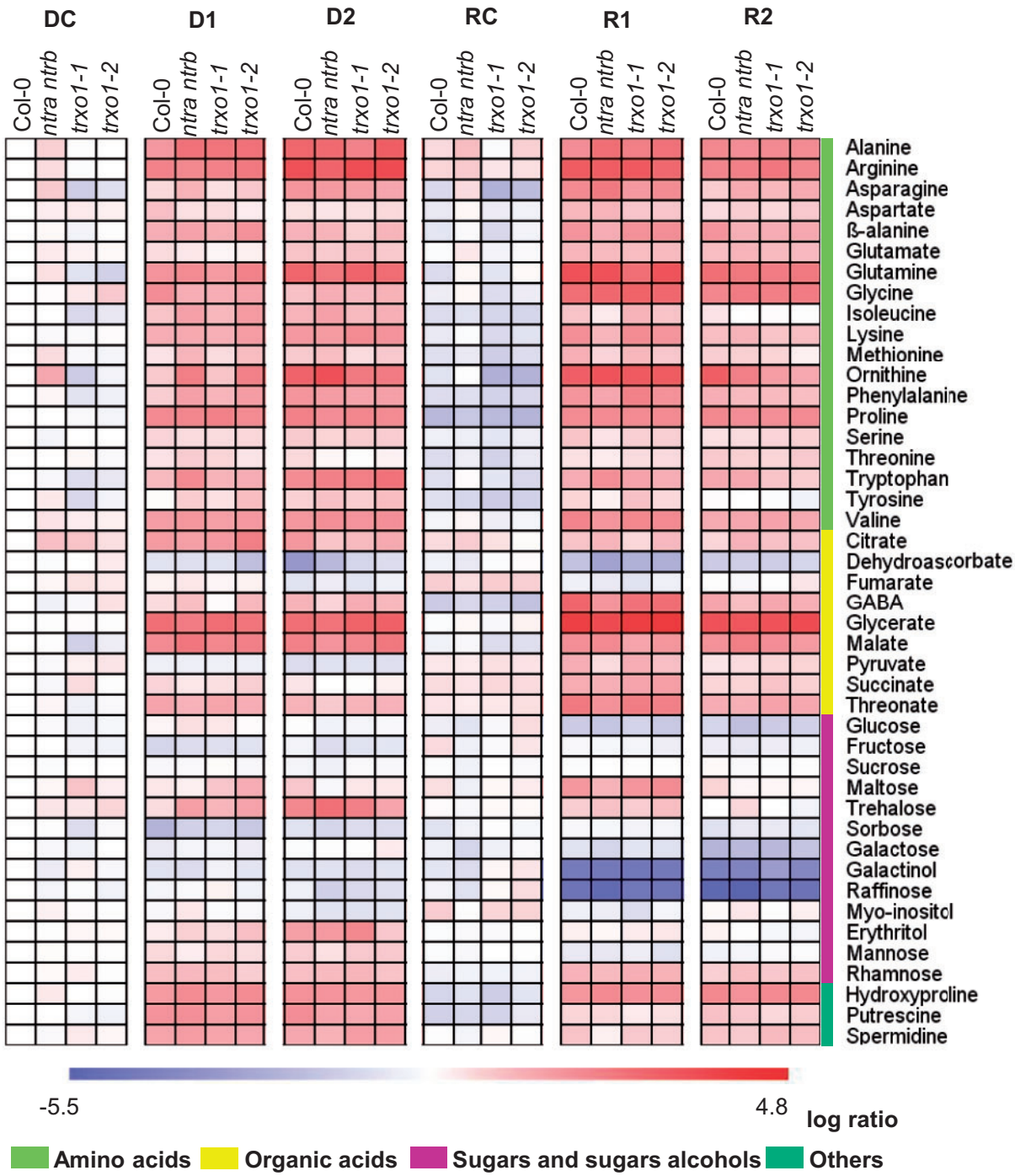

Fig. 5 Heat map representing the changes in relative abundance of primary metabolite levels in Trx Arabidopsis knockout mutants. The genotypes used here were: *ntra ntrb*, *trxo1-1* and *trxo1-2*, and wild-type plants (WT) during dehydration and following rehydration as measured by GC-MS. The heat map represents six conditions: unstressed drought control (DC), plants drought stressed only once (D1) and twice (D2), unstressed recovery control (RC) and rehydration of plants previously drought stressed once (R1) or twice (R2). Data represent averages of six biological replicates per genotype and condition, with higher relative expression in mutant lines compared with the WT in red and lower expression in blue, as indicated by the scale bar. Metabolites were determined as described in the Materials and Methods. Data are normalized with respect to the mean response calculated for the WT plants at DC.

observed higher levels of tyrosine in all the evaluated mutants and decreases in glutamate in both *ntra ntrb* and *trxo1-1* plants compared with the WT. Drought induced increases in trehalose (in all mutants), raffinose (*trxo1-1*) and *myo*-inositol (*ntra ntrb*), and reduced the levels of dehydroascorbate (DHA) (*trxo1-2*). Notably, the imposition of a second drought event resulted in alterations in a different set of metabolites. In D2, *ntra ntrb* plants displayed decreases in threonine (also in both *trxo1* lines), citrate, maltose (also in *trxo1-2*) and raffinose compared with the WT. Furthermore, both *trxo-1* lines exhibited increases

in DHA levels, whereas *trxo1-2* showed increases in tryptophan and galactose levels and *trxo1-1* showed a reduction in alanine. Lower levels of putrescine were also found in all mutants at D2.

While a similar number of primary metabolites changed in mutant plants in both drought conditions, D1 and D2, compared with the WT control, a differential response of mutant plants was revealed by liquid chromatography coupled with mass spectrometry (LC-MS) data (**Fig. 6**; Supplementary Data set IV). Thus, only the double *ntra ntrb* mutant exposed to a single drought event (D1) displayed alterations in seven secondary metabolites compared with their respective WT controls. Of these changes, only the hydroxycinnamate SinG1 was reduced, while the other six metabolites (7MSOH, 8MSOO, 4MOI3M, K3GR7R, K3G7R and K3R7R) were increased in *ntra ntrb* plants compared with their respective WT controls. In contrast, a large number of secondary metabolites significantly changed in at least one of the Trx mutant plants following two cycles of stress compared with their WT counterparts.

By analyzing primary metabolism following rewatering, it was observed that mutant plants of the R1 condition displayed changes in the levels of more metabolites than R2 plants (**Fig. 5**; Supplementary Data set III). All three Trx mutants were characterized by lower levels of DHA and higher levels of glycine and hydroxyproline under the R1 condition. Double mutant plants also exhibited decreases in threonate, a known breakdown product of ascorbate (Gechev et al. 2013), and increases in the shikimate-derived amino acid tryptophan. Accordingly, ß-alanine and GABA, non-protein amino acids, as well as methionine (also in *trxo1-2*), pyruvate, succinate, serine and spermidine, were lower in *ntra ntrb* in comparison with R1 WT plants. In addition, *trxo1-1* plants displayed lower malate and glutamate values, while both *trxo1* mutant lines presented higher alanine levels.

Minor changes were observed in the levels of primary metabolites after a second recovery event (R2). Indeed, only three metabolites were significantly reduced in R2 double *ntra ntrb* mutant plants, namely ß-alanine and maltose, which were lower in the three mutants, and threonine (which was also lower in *trxo1-1* plants). Moreover, the occurrence of a second drought/recovery cycle induced many changes in the metabolic profile of *trxo1* mutants. The levels of ornithine, erythritol and putrescine were lower in the two *trxo1* mutant lines, whereas we observed higher levels of succinate in *trxo1* lines. Higher levels of galactinol and galactose were also found compared with the WT at R2 in *trxo1-1* and *trxo1-2*, respectively.

LC-MS results (**Fig. 6**; Supplementary Data set IV) revealed an accumulation of several secondary metabolites in all mutants following both R1 and R2 conditions in Trx mutants, in comparison with the respective WT control. Interestingly, the levels of 6MTH were higher in all Trx mutants compared with the corresponding WT control in both R1 and R2 conditions, while other secondary metabolites varied in a different way in each situation (R1 or R2). For instance, the levels of the aliphatic GSLs 7MTH and 8MTH were lower in all R1 mutant plants compared with the respective WT, whereas in R2 we observed the opposite (higher levels in the mutants). Lower levels of anthocyanin were observed in double *ntra ntrb* and *trxo1-1* mutants in R1 condition and higher levels in *trxo1-2* mutants in R2, compared with their respective WT.

Differential response of pyridine nucleotide content in Arabidopsis Trx mutants during repeated drought cycles

We next decided to assay the levels of pyridine nucleotides in the six conditions evaluated here (Supplementary Fig. S6). Interestingly, *ntra ntrb* plants displayed lower levels of NAD^+ and a lower but not significant change in NADH under non-stress conditions (DC and RC), compared with the correspondent WT control, which leads to the maintenance of the NADH/NAD^+ ratio in double mutant plants (Supplementary Fig. S6). The levels of NAD^+, $NADP^+$ and NADPH substantially increased in all genotypes following the suspension of watering in both D1 and D2 conditions (Supplementary Fig. S6). Accordingly, twice drought-stressed plants (D2) displayed higher NADH levels than D1 plants. As a result, a clear pattern of reduction in the NADH/NAD^+ ratio (Supplementary Fig. S6) was observed in all D1 plants compared with both DC and D2 conditions.

Regarding the changes in NAD(P)H after rehydration, the results showed that neither the R1 nor the R2 plants fully recovered from the previous stress. Thus, the levels of NAD^+, $NADP^+$ and NADPH did not return to the levels displayed by RC plants. In addition, despite the higher NADH levels shown by D2 plants, a large decrease in NADH levels was observed after re-irrigation (R2) in such a way that RC and R2 plants exhibited relatively similar levels of NADH. Moreover, WT plants exposed to a single drought/recovery event (R1) showed greater $NADP^+$ and NAD^+ values than non-stressed WT plants (RC) or even than R2 WT plants. Consequently, all mutant plants displayed lower $NADP^+$ and NAD^+ levels compared with the respective WT (R1), which was significant only for *ntra ntrb* plants. No differences were found for NADPH/$NADP^+$ and NADH/NAD^+ ratios (Supplementary Fig. S6) between the genotypes in any of the evaluated treatments.

Gene expression in *TRX* mutant plants during repeated drought cycles

We next evaluated the transcriptional responses of select genes throughout the course of the drought cycle experiment (**Fig. 7**). Our results demonstrate a significant up-regulation of dehydration-inducible genes, especially the drought-responsive genes, *responsive to desiccation 29A* (*RD29A*), *responsive to desiccation 29B* (RD29B) and DREB2A-INTERACTING PROTEIN2 (DRIP2), in drought-stressed plants (D1 and D2). Notably, considerably higher transcript levels of RD29A and RD29B were generally found during the second drought cycle (D2) relative to D1 plants. This pattern was also observed following recovery, given the higher expression of RD29A in R2 plants compared with the R1 plants, which indicates a likely alert state in plants subjected to repeated drought episodes.

Moreover, we followed the expression pattern of the genes coding for the mitochondrial Trx system (*TRXo1*, *NTRA* and *NTRB*). Both *TRXo1* and *NTRA* were more highly expressed

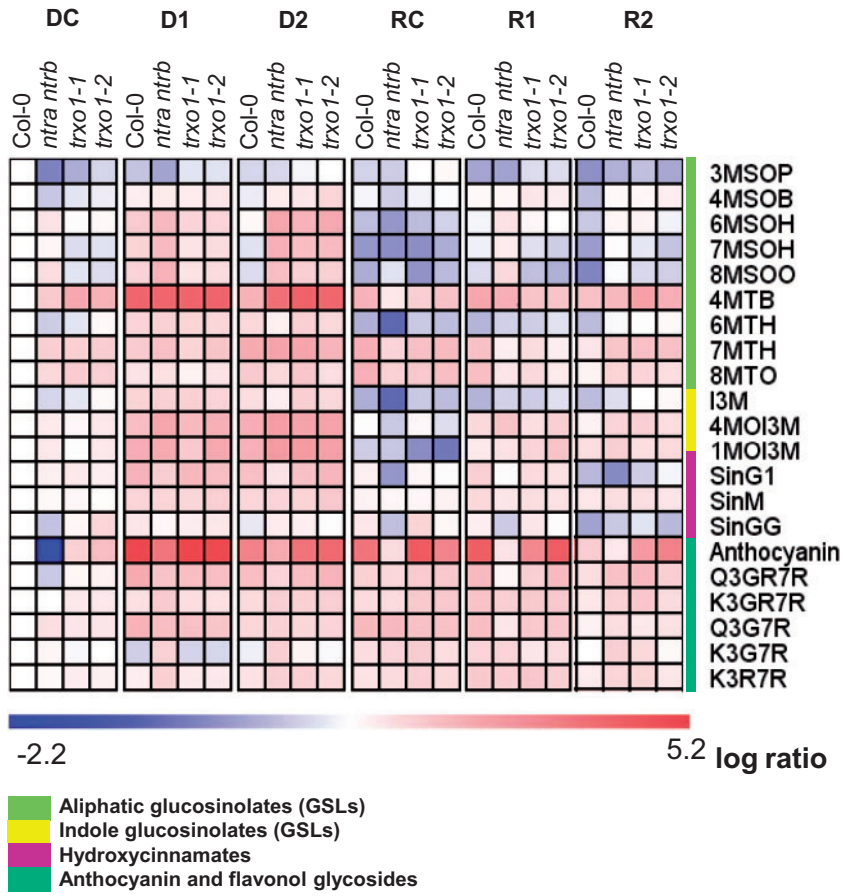

Fig. 6 Heat map representing the changes in relative abundance of secondary metabolite levels in Trx Arabidopsis knockout mutants. The genotypes used here were: *ntra ntrb*, *trxo1-1* and *trxo1-2*, and wild-type plants (WT) during dehydration and following rehydration as measured by LC-MS. The heat map represents six conditions: unstressed drought control (DC), plants drought stressed only once (D1) and twice (D2), unstressed recovery control (RC) and rehydration of plants previously drought stressed once (R1) or twice (R2). Data represent averages of six biological replicates per genotype and condition, with higher relative expression in mutant lines compared with WT in red and lower expression in blue, as indicated by the scale bar. Metabolites were determined as described in the Materials and Methods. Data are normalized with respect to the mean response calculated for the WT plants at DC. Glucosinolates: 3MSOP, 3-methylsulfinylpropyl glucosinolate; 4MSOB, 4-methylsulfinylbutyl glucosinolate; 6MSOH, 6-methylsulfinylhexyl glucosinolate; 7MSOH, 7-methylsulfinylheptyl glucosinolate; 8MSOO, 8-methylsulfinyloctyl glucosinolate; 4MTB, 4-methylthiobutyl glucosinolate; 6MTH, 6-methylthiohexyl glucosinolate; 7MTH, 7-methylthioheptyl glucosinolate; 8MTO, 8-methylthiooctyl glucosinolate; I3M, indolyl-3-methyl glucosinolate; 4MOI3M, 4-hydroxy-indolyl-3-methyl glucosinolate; 1MOI3M, 4-methoxy-indolyl-3-methyl glucosinolate. Hydroxycinnamates: SinG1, sianpoyl-*O*-glucoside; SinM, sinapoyl-malate; SinGG, sianpoyl-*O*-di-glucoside. Anthocyanin and flavonol glycosides: A11, anthocynin; Q3GR7R, quercetin-3-*O*-(2″-*O*-rhamnosyl)glucoside-7-*O*-rhamnoside; K3GR7R, kaempferol-3-*O*-(2″-*O*-rhamnosyl)glucoside-7-*O*-rhamnoside; Q3G7R, quercetin-3-*O*-glucoside-7-*O*-rhamnoside; K3G7R, kaempferol-3-*O*-glucoside-7-*O*-rhamnoside; K3R7R, keampferol-3-*O*-rhamnoside-7-*O*-rhamnoside.

following two drought cycles in WT plants (D2). Following recovery, only *NTRA* returned to the levels found prior to water stress, whereas *TRXo1* was even more induced under drought (D2) and recovery (R2) following two drought cycles. In contrast, we did not observe any changes in the expression levels of *NTRB* following drought or recovery. Although no expression of the related gene was observed for the *trxo1* (both lines *trxo1-1* and *trxo1-2*) and for *NTRB* in the double knockout, we observed only a strong reduction of *NTRA* in the double knockout compared with WT levels. Taken together, these results indicate that the genes associated with the mitochondrial Trx system seem to be highly regulated following water stress and that the down-regulation of one most probably culminated with no up-regulation of the others.

Principal component analysis reveals specific changes during drought and recovery in Trx Arabidopsis mutants

In order to gain a broad overview of the changes that occurred during drought, we subjected the data obtained from plants following cycles of drought to principal component analysis (PCA), and the first and second components were plotted (**Fig. 8**). Control (DC and RC) and drought (D1 and D2) separated mainly along PC1 (47.0% of data variability), while recovery treatments (R1 and R2) essentially resolved along PC2 (21.4% of data variability). One of the main contributors to the differences observed between control and drought plants were the higher levels of amino acids, which were clearly clustered

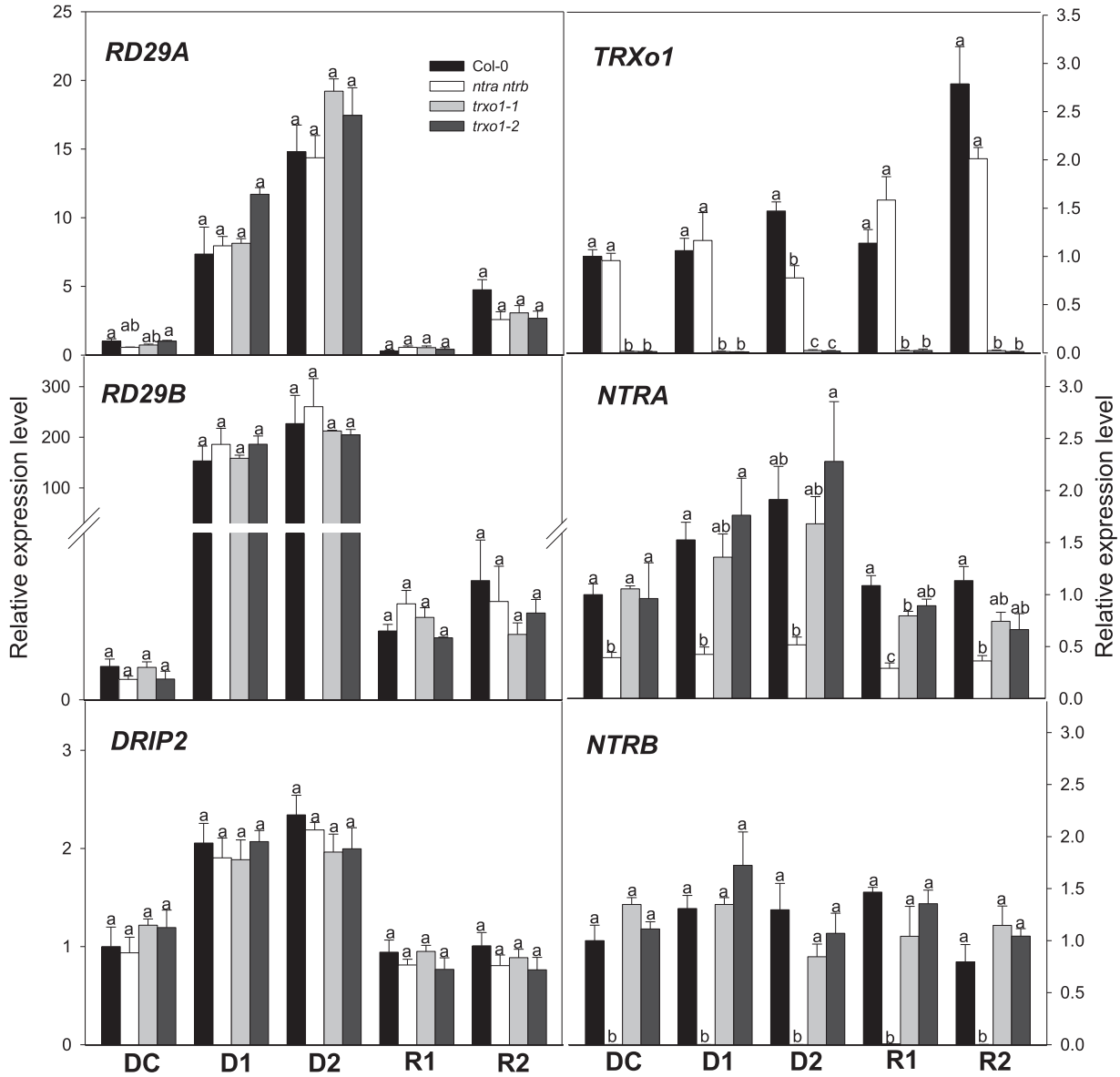

Fig. 7 Transcript levels of drought-responsive genes (*RD29A*, *RD29B* and *DRIP2*) and of genes related to mitochondrial TRX (*TRXo1*, *NTRA* and *NTRB*) in leaves of Trx Arabidopsis knockout mutants. The genotypes used here were: *ntra ntrb*, *trxo1-1*, *trxo1-2* and wild-type plants (WT) during dehydration and following rehydration. The plants were submitted to five conditions: unstressed drought control (DC), plants drought stressed only once (D1) and twice (D2) and rehydration of plants previously drought stressed once (R1) or twice (R2). F-BOX was used as an internal control. Data represent averages of four biological replicates per genotype and condition. *RD29A*, *responsive to desiccation 29A*; *RD29B*, *responsive to desiccation 29B*; and *DRIP2*, DREB2A-INTERACTING PROTEIN2 (DRIP2). Different letters represent values that that were judged to be statistically different between treatments by Tukey's multiple comparison test ($P < 0.05$).

(Supplementary Fig. S7; Supplementary Table S3). Interestingly, the compatible solutes proline and hydroxyproline were the main determinants of PC1. Both proline and hydroxyproline increased after drought (D1 and D2) and were kept higher following recovery for all the genotypes compared with the control (DC) (**Fig. 5**; Supplementary Data set III). However, proline levels in all mutants do seem to be different from those in the the WT, whereas hydroxyproline was significantly up-regulated in all mutants at R1 compared with their WT counterparts (**Fig. 5**; Supplementary Data set III). The increases in the aromatic amino acids, tyrosine, tryptophan and phenylalanine, as well as in the BCAAs valine and isoleucine were also remarkable within PC1 where they, as well as lysine, serine and alanine, provide a massive contribution to sample separation (Supplementary Fig. S7; Supplementary Table S3). In contrast, higher levels of GABA and glycine, as well as the strong reductions in glucose, raffinose and galactinol following recovery compared with drought and control plants are seemingly of great importance for the separation observed within PC2.

Discussion

Several suitable physiological, metabolic and biochemical adjustments are required in order to allow plants to support

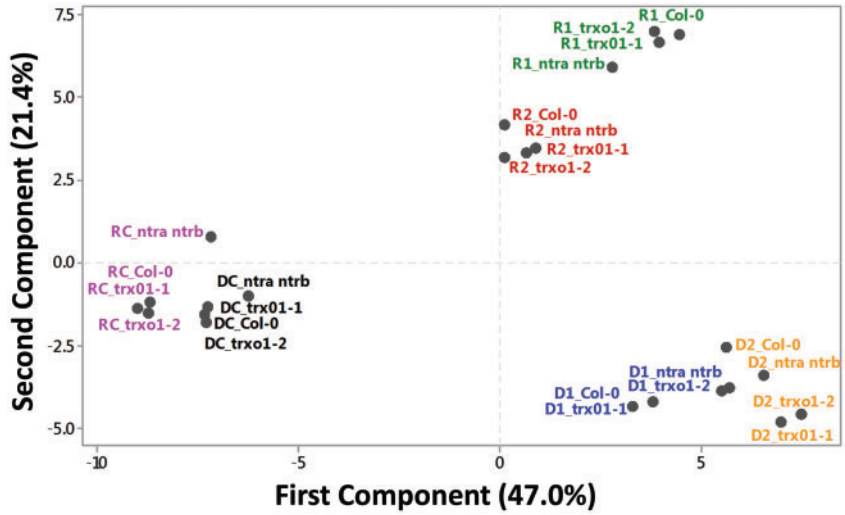

Fig. 8 Principal component analysis (PCA) of metabolic and growth parameter data. PCA was performed on the correlation matrix of least square means. Numbers in parentheses give the percentage variation explained by the first and the second components, which together comprise 68.4% of the total variance. The six treatments are indicated by different colors: unstressed drought control (DC) in black, plants drought stressed only once (D1) in blue and twice (D2) in orange, unstressed recovery control (RC) in pink and rehydration of plants previously drought stressed once (R1) or twice (R2) in green and red, respectively. The colored circles represent the cluster formed by Pearson distance.

growth and development under drought. Although the connection between drought and redox metabolism has been demonstrated, our current understanding of the metabolic process associated with mitochondrial redox proteins under stress remains fragmentary. Thus, here we investigated the acclimation responses of mitochondrial *TRX* mutant plants exposed to drought conditions. By using well-characterized mutants with reduced expression of the mitochondrial Trx system, we observed that these mutants were able to better recover the values of the well-established stress-related F_v/F_m parameter than WT plants after exposure to a single drought event (**Fig. 1C**). Metabolic changes provide evidence that the absence of a functional mitochondrial Trx system leads to a complex metabolic reprogramming following dehydration stress (**Figs. 2, 3, 5, 6**). Our data also suggest that the mutants most probably displayed a faster recovery due to the operation of other cellular mechanisms in order to compensate the lack of the mitochondrial Trx system and simultaneously maintain cell homeostasis under drought. Our data are thus in good agreement with recent reports which demonstrate that higher activities of antioxidative enzymes are able to counteract *TRXo1* deficiency in Arabidopsis mutant plants under salinity (Ortiz-Espín et al. 2017, Calderón et al. 2018).

It has been shown that plants are able to fortify their defenses by retaining information from previous stress experiences (Crisp et al. 2016). In good agreement with this, Trx mutants that experienced two cycles of water limitation (D2 plants) responded to water shortage with a significantly higher F_v/F_m (**Fig. 4C**) and a better visual phenotypic appearance than their counterparts that experienced drought once only (**Fig. 4A**). Moreover, the levels of sucrose were higher during drought (D1 and D2), but they returned to the levels found prior to water stress following re-irrigation in all genotypes studied here (Supplementary Fig. S4). In contrast, starch levels were virtually depleted after withholding water and were not restored to the values observed under the control condition (Supplementary Fig. S4). Photosynthetic rates (A_N) following re-watering were also not fully recovered at R2 in all genotypes evaluated here, despite the similar values of F_v/F_m observed for all genotypes (Supplementary Table S2). Taken together, these results indicate that stressed plants were not able to recover fully after water limitation.

PCA of the drought cycle experiment revealed that the mutant and WT plants clustered together (**Fig. 8**), confirming that the metabolic changes triggered by the drought condition followed the same pattern for all genotypes, albeit more pronounced in the mutants (**Figs. 5, 6**). The consistent accumulation of aromatic amino acids in both drought experiments (single and shared pots; **Figs. 2 and 5**, respectively) probably indicates activation of the phenylpropanoid pathway under water limitation (Dinakar and Bartels 2013, Gechev et al. 2013, Jorge et al. 2016). Indeed, larger increases were found in the major classes of secondary metabolites derived from phenylalanine, tyrosine and tryptophan in drought-stressed mutant plants than in their WT counterparts (**Fig. 6**; Supplementary Data set IV). These results are consistent with the previous demonstration that flavonoid biosynthesis genes and the total flavonoid accumulation are induced in a co-ordinated manner in the *ntra ntrb* double mutant (Bashandy et al. 2009), and reinforce the idea that secondary metabolism is also subjected to a Trx-mediated redox regulation (Daloso et al. 2015). In fact, it is highly possible that NTRs act on flavonoid biosynthesis through one or several of the cytosolic and/or mitochondrial Trx or Trx-like proteins that are encoded in the Arabidopsis genome (Bashandy et al. 2009). However, despite this evidence, 3-deoxy-D-*arabino*-heptulosonate 7-phosphate (DAHP) synthase, an enzyme of the shikimate pathway, has been the only enzyme of secondary

metabolism demonstrated to be regulated by Trxs (Entus et al. 2002). Future studies are clearly required to identify further Trx targets from secondary metabolism and to dissect how and to what extent Trxs co-ordinate the flux through this pathway.

The results of our secondary metabolism profiles from D1 and D2 plants indicate that a much greater number of changes were displayed by Trx mutants subjected to two periods of drought stress (D2) when compared with Trx plants subjected to a single period of drought stress (D1) and with their WT controls (**Fig. 6**; Supplementary Data set IV). This is consistent with the hypothesis that plants are able to incorporate relevant information from previous stress experiences (Trewavas 2003, Hilker et al. 2016, Menezes-Silva et al. 2017). The results are in good agreement with the clear higher induction of RD29A and RD29B during the second drought cycle (D2) (**Fig. 7**), confirming the existence of differential molecular adjustments in D2 plants. It is important to note the alterations in the aromatic sinapoyl-malate (SinM), whose contribution to PC1 was much larger than the average contribution of the other secondary metabolites identified here (Supplementary Fig. S7; Supplementary Table S3). SinM is the main sinapate ester in Arabidopsis leaves (König et al. 2014), often described as a classical UV-B screening agent (Dean et al. 2014, Jorge et al. 2016). However, SinM also seems to be associated with drought tolerance in plants (Mattana et al. 2005, Valliyodan and Nguyen 2006). Not only the increase in amino acid and SinM levels but also other adaptive mechanisms including the accumulation of trehalose (**Fig. 2**; Supplementary Data set I), the polyamines spermidine and putrescine (**Fig. 2**) and hydroxyproline (**Figs. 2, 5**) seem to be of pivotal importance during drought episodes. Accordingly, increases in the levels of all these metabolites have previously been shown to confer drought protection (Cramer et al. 2007, Urano et al. 2009, Cramer et al. 2013, Do et al. 2013, Jorge et al. 2016) and as such might be associated with the enhanced performance of Trx mutants following drought. On the other hand, decreases in DHA levels in the Trx mutants in comparison with WT counterparts at R1 (**Fig. 5**; Supplementary Data set III) may suggest alterations in the redox status in these plants, which does not seem to be the case given the absence of differences for $NADPH/NADP^+$ and $NADH/NAD^+$ ratios (Supplementary Fig. S6) between the genotypes in any of the evaluated treatments. Interestingly, tobacco mutant plants overexpressing DHAR (dehydroascorbate reductase) were characterized by lower levels of hydrogen peroxide and DHA in comparison with WT plants, also displaying an increased g_s (Gallie 2013), which suggests that the lower DHA levels found in Trx mutants (R1) are most likely to be associated with the better recovery of g_s in the mutants. Furthermore, we did not observe any evidence of compensation at the expression level of NTR/Trx o1 genes in the mutants investigated here under control conditions (**Fig. 7**). In contrast, Trx o1 expression was reduced in the *ntra ntrb* double mutant in D2 plants (**Fig. 7**). Indeed, several other components of redox metabolism such as glutathione-related enzymes (e.g. glutaredoxins) may be able to compensate the absence of mitochondrial NTR/Trx enzymes. In fact glutathione has been suggested to play a major role in drought stress acclimation (Cheng et al. 2015) and to operate as a backup system for TRX (Reichheld et al. 2007, Marty et al. 2009, Bashandy et al. 2010). Therefore, re-adjustment of glutathione levels and/or the redox state as well as increased activity of glutathione-related enzymes might also be involved in the more complete recovery of *trxo1* and *ntra ntrb* mutants after drought stress, similar to the situation observed in *trxo1* mutants under salt stress (Calderón et al. 2018). However, analysis of this possibility was beyond the scope of the present study and thus remains to be fully investigated.

The higher contribution of the organic acids pyruvate and succinate—metabolites which generally increased in both recovery treatments (R1 and R2) in all genotypes—along with the increase in GABA and in the photorespiratory intermediates glycine and glycerate, three metabolites which increased during drought (D1 and D2) and even more following recovery, were associated with the changes observed in our PCA (**Fig. 8**; Supplementary Fig. S7; Supplementary Table S3). The GABA shunt has been associated with energetic stress situations, and therefore the changes observed are suggestive that Trx mutants are adjusting their metabolism via changes in the GABA-related compounds, in order to support energy production (Fait et al. 2008). This would allow the mutants to better cope with the drought and particularly with recurrent events of water limitation. In turn, the reduction in the abundance of glucose and mannose together with the accumulation of pyruvate in all genotypes suggests the activation of the glycolytic pathway during recovery (Yobi et al. 2013, Jorge et al. 2016). In addition, the decrease in monosaccharides is linked to the increased production of sucrose (Gechev et al. 2013). However, our data demonstrate a decrease in sucrose following recovery (R1 and R2) compared with the levels observed under drought conditions (D1 and D2) (Supplementary Fig. S5), suggesting the existence of a co-regulation between glycolysis and sucrose metabolism during drought recovery. Similar apparent contrasting metabolite changes have been previously found in response to salt stress and might be attributed to the complex adaptation of soluble osmolytes (Obata and Fernie 2012, Jorge et al. 2016). The pronounced down-regulation of raffinose and galactinol on recovery indicates that flux was probably redirected to more energetically favorable pathways.

Although our results are not able to elucidate fully the metabolic complexity behind successive drought events, it seems that by affecting mitochondrial redox metabolism plants are better able to cope with such a situation. We postulate that this is linked to a lower energetic expenditure that would allow a faster recovery in Trx mutants. Collectively, our results are consistent with a complex metabolic reprogramming of the main pathways of primary and secondary metabolism to maintain a fine-tuned and balanced energetic metabolism during drought and recovery. We further demonstrate the existence of a drought memory effect, as observed by the reduced number of changes and a closer metabolic situation in twice-stressed plants (R2) compared with control plants. Perhaps more importantly, we also observed that *trx* mutant plants are less sensitive to such recurrent events and postulate that this is

due to a redox-based metabolic reprogramming. It seems likely that a differential and orchestrated response occurred in the mutants, which affected primary and secondary metabolic pathways and ultimately resulted in alterations in the redox poise following recovery. Thus, increasing our understanding of how Trxs interact to allow interorganellar communication will provide us with a more comprehensive picture of redox modulation of both plant growth and metabolism under such conditions. It seems reasonable to assume that the generation of multiple mutants for Trx and glutaredoxin genes localized in different cell compartments will enhance our knowledge of both specificities and redundancies of these different albeit partially complementary redox systems (Geigenberger et al. 2017), allowing us truly to understand the molecular hierarchy under which they operate.

Materials and Methods

Growth conditions and experimental design

All *Arabidopsis thaliana* plants were of the Columbia ecotype (Col-0) background. The *ntra ntrb* double knockout mutant was previously described (Reichheld et al. 2007), whereas the two T-DNA insertion mutants in the *trxo1* gene (At2g35010) from the Salk collection, *trxo1-1* (SALK_042792) and *trxo1-2* (SALK_143294), were described by Ortiz-Espín et al. (2017). Homozygous lines for each mutant were characterized by genomic PCR (Supplementary Fig. S1). Real-time PCR (RT-PCR) using primer pairs designed to span the T-DNA insertion sites of the two mutant loci was used to investigate transcription of both *TRXo1-1* and *TRXo1-2* (Supplementary Fig. S1). The Arabidopsis *TRXh5* was used as a control to demonstrate the integrity of the RNA preparation. *TRXo1-1* and *TRXo1-2* mRNAs were detected in the WT (Col-0) using the set of primers 1 (CTCGAGTGATGAAGGGAAATTGGTCG) and 3 (CAACACGTTCTTTACTAGAACGG); however, no amplification products were observed for the transcripts in *trxo1-1* and *trxo1-2* (Supplementary Fig. S1). The seeds of the four genotypes used (Col-0, *ntra ntrb*, *trxo1-1* and *trxo1-2*) were sown on standard greenhouse soil (Stender) in plastic pots with a 0.5 liter capacity. The trays containing the pots were placed under a 12/12 h day/night cycle (22/16°C) with 60/75% relative humidity and 150 µmol photons m^{-2} s^{-1} light intensity. At 14 d after sowing, plants were transferred to single pots (0.1 liter), which were placed in a random arrangement in the tray and then transferred to climate chambers with a 8/16 h day/night cycle (22/16°C, 60/75% relative humidity and 150 µmol photons m^{-2} s^{-1} light intensity). One month after the transfer to single pots, plants were subjected to a progressive water deficit by suspension of irrigation and then given recovery irrigation. At days 0, 5 and 10 of drought stress and following 3 d of recovery irrigation, the RWC and the F_v/F_m were determined and whole rosettes were harvested at around 4 h in the light (middle of the photoperiod) for further analysis. Control plants were watered daily and kept under well-watered conditions throughout the whole stress/recovery period.

We additionally grew plants side-by-side in a similar manner in large plastic pots with a 0.5 liter capacity to allow comparison of the responses in similar soil conditions and to be confident that the water restriction was identical in all genotypes. To this end, 14 d after sowing, plants were transferred to large pots where there was one plant representing each genotype and kept in climate chambers with similar conditions to those described above. One month after the transfer to large pots, plants were divided into three groups. One group was watered daily during the entire experiment including the stress/recovery period (control plants). The second group was subjected to one drought event, followed by a recovery (D1 plants). The third group was submitted to two drought events intercalated with drought recovery periods (D2 plants). The plants subjected to drought events (D1 and D2) and their respective control plants (DC) were all harvested at the same age [at 51 days after sowing (DAS), as indicated by dotted blue lines in Supplementary Fig. S2]. Similarly, the plants subjected to the recovery irrigation (R1 and R2) and their respective controls (RC) were all evaluated at the same age (at 54 DAS). Moreover, plants from R2 treatments were subjected to two recurrent episodes of rehydration, each one after a 10 d period of drought, while plants from R1 were exposed just once to drought (for 10 d) and recovery (for 3 d). Both experiments were repeated at least twice (and even in different growth facilities) with similar phenotypes observed on each occasion.

Relative water content (RWC)

Leaf RWC was assessed to monitor the status of leaf hydration. One leaf from each replicate was excised and weighed in order to obtain the fresh weight (FW). Afterwards, leaves were hydrated for 2 h in a Petri dish containing distilled water, under greenhouse conditions, and weighed in order to obtain the turgid weight (TW). Finally, leaves were oven-dried at 72°C for 72 h and weighed in order to obtain the dry weight (DW). For the calculation of RWC, the following equation was used: RWC = (FW − DW)/(TW − DW).

Chl *a* fluorescence imaging

Fluorescence imaging parameters were determined by using the Imaging-PAM M-Series Chl fluorometer and the software version 2.32 Imaging WIN (both from Heinz Walz GmbH). Plants were adapted to darkness for at least 30 min, then the leaves were exposed to a light pulse intensity of 0.5 µmol m^{-2} s^{-1} (1 Hz) to establish the minimum fluorescence image (F_0). Next, a saturating pulse of actinic light (470 nm) of 2,400 µmol m^{-2} s^{-1} intensity (10 Hz) was delivered during 0.8 s in order to obtain the maximum fluorescence image (F_m). Thereafter, the calculation of the maximum quantum efficiency of PSII used the formula $F_v/F_m = (F_m - F_0)/F_m$. For semi-quantitative analyses, 15 areas of interest of 1 cm^2 each were randomly sampled on the image of each leaf. For each parameter, six individual plants were used and the values obtained were averaged.

Gas exchange and Chl *a* fluorescence measurements

These physiological *in vivo* measurements were performed in the second experiment. One plant of each line and a WT were grown in the same pot (as described previously) taking into account previous considerations to facilitate *in vivo* gas exchange measurements in the leaves of the growing Arabidopsis rosettes through the 'ice-cream cone-like' soil pot method (Flexas et al. 2007). Leaves (the sixth to eighth pair of the rosette) were labeled to perform gas exchange measurements during the whole experiment. Gas exchange parameters were determined simultaneously with Chl *a* fluorescence measurements using an open-flow infrared gas exchange analyzer system (LI-6400XT; LI-COR) equipped with an integrated fluorescence chamber (LI-6400-40; LI-COR). Instantaneous gas exchange data were obtained after the steady state was reached (40–60 min) under light saturation conditions [1,000 µmol photons m^{-2} s^{-1} at the leaf level, while the amount of blue light was set to 10% photosynthetically active photon flux density (PPFD) to optimize stomatal aperture]. The reference CO_2 concentration was set at 400 µmol CO_2 mol^{-1} air. All measurements were performed using the 2 cm^2 leaf chamber maintaining the block temperature at 25°C, the leaf-to-air vapor pressure deficit was kept at 1.5–2.5 kPa and flow rates ranging from 100 to 300 mmol air min^{-1} (depending on gas exchange rates, flow was reduced to ensure maximum precision in the equipment following previous recommendations; Gago et al. 2013). Cuvette chamber leakage was corrected as described previously in Flexas et al. (2007). The very low gas exchange rates under drought conditions did not allow us to perform precise measurements with the equipment (ΔCO_2 <0.5 in a flow of 100 µmol mol^{-1} air). The same plants used for photosynthesis measurements were darkened for a minimum of 60 min (at the end of the day) to measure mitochondrial respiration in the dark (R_{dark}); the light non-photorespiratory CO_2 release (R_{light}) was considered as half of R_{dark} (Niinemets et al. 2005). The photorespiration rate (P_r) was calculated following the model based on gas exchange and Chl fluorescence measurements proposed by Valentini et al. (1995).

In parallel to the gas exchange measurements, Chl *a* fluorescence recordings were used to calculate the actual photochemical efficiency of PSII, φPSII = (*Fm*'–*Fs*)/*Fm*', where F_s is the steady-state fluorescence and F_m' is the maximum fluorescence obtained with a saturation pulse of approximately 8,000 µmol m^{-2} s^{-1}

(Genty et al. 1989). As the φPSII represents the number of electrons transferred per photon absorbed in PSII, the electron transport rate (ETR) was calculated as $ETR = \varphi PSII \times \alpha \times ß \times PAR_i$, where α is leaf absorbance, ß reflects the partitioning of absorbed quanta between PSII and PSI, and PAR_i is the incident photosynthetically active radiation on the leaf surface. The relationship between φPSII and φCO_2 under non-photorespiratory conditions was used to calculate the product $\alpha \times ß$ (Valentini et al. 1995). Mesophyll conductance (g_m) was estimated using the method established by Harley et al. (1992). In this method, g_m was estimated using the following equation $g_m = A_N / (C_i - (\Gamma^* (J_{flu} + 8(A_N + R_d)) / (J_{flu} - 4(A_N + R_d))))$. All parameters, except the CO_2 compensation point (Γ^*), were estimated as described above, and Γ^* was calculated from *in vitro* determinations of $S_{C/O}$, as $\Gamma^* = 0.5 \times O / S_{C/O}$ (Caemmerer 2000).

Determination of metabolite levels

Whole rosettes were sampled at the indicated time points, immediately frozen in liquid nitrogen, and stored at −80°C until further analysis. Metabolite extraction was performed by rapid grinding in liquid nitrogen and immediate addition of the appropriate extraction buffer. The levels of starch, sucrose, fructose and glucose in the leaf tissues were determined exactly as described previously (Fernie et al. 2001). Malate and fumarate were determined exactly as in Nunes-Nesi et al. (2007). Proteins and amino acids were determined as described previously (Cross et al. 2006). Nitrate was determined as detailed in Sienkiewicz-Porzucek et al. (2010).

Metabolite profiling was determined by GC-MS (primary metabolites) (Lisec et al. 2006) and LC-MS (secondary metabolites) (Tohge and Fernie 2010). Metabolites were identified by comparison with database entries of authentic standards (Kopka et al. 2005, Schauer et al. 2005). Chromatograms and mass spectra were evaluated by using Chroma TOF 1.0 (Leco, http://www.leco.com/) and TAGFINDER 4.0 software (Luedemann et al. 2008). The relative content of metabolites was calculated by normalization of signal intensity to that of ribitol, which was added as an internal standard, and then by dry weight of the material. Secondary metabolite analysis by LC-MS was performed as described (Tohge and Fernie 2010). All data were processed using Xcalibur 2.1 software (Thermo Fisher Scientific). The obtained data matrix of peak area was normalized using the internal standard (isovitexin, CAS: 29702-25-8) and then by dry weight of the material. Metabolite identification and annotation were performed using metabolite databases (Tohge and Fernie 2009). Identification and annotation of detected peaks followed the recommendations for reporting metabolite data described in Fernie et al. (2011). The full data set from GC-MS and LC-MS metabolite profiling, including statistical analysis performed as described below, are available as Supplementary Data sets I–IV.

Determination of pyridine nucleotides

The procedures used to assay pyridine nucleotides were based on the selective hydrolysis of the reduced forms (NADH and NADPH) in acid medium, and of the oxidized forms (NAD^+ and $NADP^+$) in alkaline medium (Hajirezaei et al. 2002). Pyridine nucleotides were assayed using the phenazine methosulfate-catalyzed reduction of dichlorophenolindophenol in the presence of ethanol and alcohol dehydrogenase (for NAD^+ and NADH) or glucose 6-phosphate (G6P) and G6P dehydrogenase (for $NADP^+$ and NADPH) (Queval and Noctor 2007).

Expression analysis by quantitative RT-PCR

Total RNA was isolated using TRIzol reagent (Ambion, Life Technology) according to the manufacturer's recommendations. The total RNA was treated with DNase I (RQ1 RNase-free DNase I, Promega). The integrity of the RNA was checked on 1% (w/v) agarose gels, and the concentration was measured using a Nanodrop spectrophotometer. Finally, 2 μg of total RNA were reverse transcribed with Superscript II RNase H2 reverse transcriptase (Invitrogen) and oligo(dT) primer according to the manufacture's recommendations. Quantitative RT-PCR was performed in a 96-well plate with an ABI PRISM 7900 HT sequence detection system (Applied Biosystems Appllera), using Power SYBR Green PCR Master Mix according to Piques et al. (2009).

The primers used here were designed using the open-source program QuantPrime-qPCR primer designed tool (Arvidsson et al. 2008) The relative transcription abundance was normalized using the constitutively expressed gene FBOX (At5g15710) calculated using the ΔΔCT method. The primers used for quantitative RT-PCR were designed using the QuantPrime software (Arvidsson et al. 2008). The primers that were used here are described in Supplementary Table S1. Data analyses were performed as described by Caldana et al. (2007). Four biological replicates were analyzed for each condition.

Statistical analysis

The experiments were conducted in a completely randomized design with 6–8 replicates of each genotype. Data were statistically examined by one-way analysis of variance (ANOVA) and Tukey's test ($P < 0.05$) using the free software R (2017) with LATTICE library. In order to reduce the dimensionality of the data set and identify the variables that explained a higher proportion of the total variance, a multivariate analysis by PCA was used in the Minitab® 17 statistics program (Minitab Inc.). We also used the Thompson tau methods with mean and median to eliminate outliers (Cimbala 2011), which are data that are statistically inconsistent with the rest of the data.

Supplementary Data

Supplementary data are available at PCP online.

Funding

This work was supported by the Max Planck Society; the CNPq (National Council for Scientific and Technological Development, Brazil) [grant No. 402511/2016-6, a scholarship to J.A.C.A. and research fellowships to A.N.N., D.M.D. and W.L.A.]; the FAPEMIG (Foundation for Research Assistance of the Minas Gerais State, Brazil [grant Nos. APQ-01078-15, APQ-01357-14 and RED-00053-16, and a scholarship to F.M.O.S.]; CAPES (Coordination for the Improvement of Higher Education Personnel, Brazil) [scholarship to P.F.P.]; and the Spanish Government [the research program 'Juan de la Cierva' post-doc grant to J.G.].

Acknowledgments

The authors acknowledge Ina Krahnert (Max Planck Institute of Molecular Plant Physiology-MPIMP) for helpful technical support.

Disclosures

The authors have no conflicts of interest to declare.

References

Anjum, N.A., Khan, N.A., Sofo, A., Baier, M. and Kizek, R. (2016) Redox homeostasis managers in plants under environmental stresses. *Front. Environ. Sci.* 4: 1–3.

Arbona, V., Manzi, M., de Ollas, C. and Gómez-Cadenas, A. (2013) Metabolomics as a tool to investigate abiotic stress tolerance in plants. *Int. J. Mol. Sci.* 14: 4885–4911.

Arvidsson, S., Kwasniewski, M., Riaño-Pachón, D.M. and Mueller-Roeber, B. (2008) QuantPrime—a flexible tool for reliable high-throughput primer design for quantitative PCR. *BMC Bioinformatics* 9: 465.

Balmer, Y., Vensel, W.H., Tanaka, C.K., Hurkman, W.J., Gelhaye, E., Rouhier, N., et al. (2004) Thioredoxin links redox to the regulation of

fundamental processes of plant mitochondria. *Proc. Natl. Acad. Sci. USA* 101: 2642–2647.

Bashandy, T., Taconnat, L., Renou, J.P., Meyer, Y. and Reichheld, J.P. (2009) Accumulation of flavonoids in an ntra ntrb mutant leads to tolerance to UV-C. *Mol. Plant.* 2: 249–258.

Bashandy, T., Guilleminot, J., Vernoux, T., Caparros-Ruiz, D.Ljung, K., Meyer, Y. et al. (2010) Interplay between the NADP-linked thioredoxin and glutathione systems in Arabidopsis auxin signaling. *Plant Cell* 22: 376–391.

Buchanan, B.B. (1980) Role of light in the regulation of chloroplast enzymes. *Annu. Rev. Plant Physiol.* 31: 341–374.

Caemmerer, S.V. (2000) Biochemical models of leaf photosynthesis. *Tech. Plant Sci.* 53: 1689–1699.

Caldana, C., Scheible, W.-R., Mueller-Roeber, B. and Ruzicic, S. (2007) A quantitative RT-PCR platform for high-throughput expression profiling of 2500 rice transcription factors. *Plant Methods* 3: 7.

Calderón, A., Sánchez-Guerrero, A., Ortiz-Espín, A., Martínez-Alcalá, I., Camejo, D., Jiménez, A., et al. (2018) Lack of mitochondrial thioredoxin o1 is compensated by antioxidant components under salinity in *Arabidopsis thaliana* plants. *Physiol. Plant.* 164:251–267.

Cattivelli, L., Rizza, F., Badeck, F.W., Mazzucotelli, E., Mastrangelo, A.M., Francia, E., et al. (2008) Drought tolerance improvement in crop plants: an integrated view from breeding to genomics. *Field Crops Res.* 105: 1–14.

Cha, J.-Y., Barman, D.N., Kim, M.G. and Kim, W.-Y. (2015) Stress defense mechanisms of NADPH-dependent thioredoxin reductases (NTRs) in plants. *Plant Signal. Behav.* 10: e1017698.

Cha, J.Y., Kim, J.Y., Jung, I.J., Kim, M.R., Melencion, A., Alam, S.S., et al. (2014) NADPH-dependent thioredoxin reductase A (NTRA) confers elevated tolerance to oxidative stress and drought. *Plant Physiol. Biochem.* 80: 184–191.

Chae, H.B., Moon, J.C., Shin, M.R., Chi, Y.H., Jung, Y.J., Lee, S.Y., et al. (2013) Thioredoxin reductase type C (NTRC) orchestrates enhanced thermotolerance to arabidopsis by its redox-dependent holdase chaperone function. *Mol. Plant* 6: 323–336.

Cheng, M.C., Ko, K., Chang, W.L., Kuo, W.C., Chen, G.H. and Lin, T.P. (2015) Increased glutathione contributes to stress tolerance and global translational changes in Arabidopsis. *Plant J.* 83: 926–939.

Cimbala, J.M. (2011) Outliers, Vol. 84. Penn State—A Public Research University, Department of Mechanical and Nuclear Engineering.

Correa-Aragunde, N., Cejudo, F.J. and Lamattina, L. (2015) Nitric oxide is required for the auxin-induced activation of NADPH-dependent thioredoxin reductase and protein denitrosylation during root growth responses in Arabidopsis. *Ann. Bot.* 116: 695–702.

Cramer, G.R., Ergül, A., Grimplet, J., Tillett, R.L., Tattersall, E.A.R., Bohlman, M.C., et al. (2007) Water and salinity stress in grapevines: early and late changes in transcript and metabolite profiles. *Funct. Integr. Genomics* 7: 111–134.

Cramer, G.R., Van Sluyter, S.C., Hopper, D.W., Pascovici, D., Keighley, T. and Haynes, P.A. (2013) Proteomic analysis indicates massive changes in metabolism prior to the inhibition of growth and photosynthesis of grapevine (*Vitis vinifera* L.) in response to water deficit. *BMC Plant Biol.* 13: 1–22.

Crisp, P.A., Ganguly, D., Eichten, S.R., Borevitz, J.O. and Pogson, B.J. (2016) Reconsidering plant memory: intersections between stress recovery, RNA turnover, and epigenetics. *Sci. Adv.* 2: e1501340.

Cross, J.M., Korff, M., Von Altmann, T., Bartzetko, L., Sulpice, R., Gibon, Y., et al. (2006) Variation of enzyme activities and metabolite levels in 24 Arabidopsis accessions growing in carbon-limited conditions. *Plant Physiol.* 142: 1574–1588.

Daloso, D.M., Müller, K., Obata, T., Florian, A., Tohge, T., Bottcher, A., et al. (2015) Thioredoxin, a master regulator of the tricarboxylic acid cycle in plant mitochondria. *Proc. Natl. Acad. Sci. USA* 112: E1392–E1400.

Dean, J.C., Kusaka, R., Walsh, P.S., Allais, F. and Zwier, T.S. (2014) Plant sunscreens in the UV-B: ultraviolet spectroscopy of jet-cooled sinapoyl malate, sinapic acid, and sinapate ester derivatives. *J. Amer. Chem. Soc.* 136: 14780–14795.

Dinakar, C. and Bartels, D. (2013) Desiccation tolerance in resurrection plants: new insights from transcriptome, proteome and metabolome analysis. *Front. Plant Sci.* 4: 482.

Ding, Y., Fromm, M. and Avramova, Z. (2012) Multiple exposures to drought 'train' transcriptional responses in Arabidopsis. *Nat. Commun.* 3: 740.

Ding, Y., Liu, N., Virlouvet, L., Riethoven, J.-J., Fromm, M. and Avramova, Z. (2013) Four distinct types of dehydration stress memory genes in *Arabidopsis thaliana*. *BMC Plant Biol.* 13: 229.

Ding, Y., Virlouvet, L., Liu, N., Riethoven, J.-J., Fromm, M. and Avramova, Z. (2014) Dehydration stress memory genes of *Zea mays*; comparison with *Arabidopsis thaliana*. *BMC Plant Biol.* 14: 141.

Do, P.T., Degenkolbe, T., Erban, A., Heyer, A.G., Kopka, J., Köhl, K.I., et al. (2013) Dissecting rice polyamine metabolism under controlled long-term drought stress. *PLoS One* 8: e60325.

Entus, R., Poling, M. and Herrmann, K. (2002) Redox regulation of Arabidopsis 3-deoxy-D-arabino-heptulosonate 7-phosphate synthase. *Plant Physiol.* 129: 1866–1871.

Fait, A., Fromm, H., Walter, D., Galili, G. and Fernie, A.R. (2008) Highway or byway: the metabolic role of the GABA shunt in plants. *Trends Plant Sci.* 13: 14–19.

Fernie, A.R., Aharoni, A., Willmitzer, L., Stitt, M., Tohge, T., Kopka, J., et al. (2011) Recommendations for reporting metabolite data. *Plant Cell* 23: 2477–2482.

Fernie, A.R., Roscher, A., Ratcliffe, R.G. and Kruger, N.J. (2001) Fructose 2,6-bisphosphate activates pyrophosphate: fructose-6-phosphate 1-phosphotransferase and increases triose phosphate to hexose phosphate cycling heterotrophic cells. *Planta* 212: 250–263.

Flexas, J., Ortuño, M.F., Ribas-Carbo, M., Diaz-Espejo, A., Flórez-Sarasa, I.D. and Medrano, H. (2007) Mesophyll conductance to CO_2 in *Arabidopsis thaliana*. *New Phytol.* 175: 501–511.

Gago, J., Coopman, R.E., Cabrera, H.M., Hermida, C., Molins, A., Conesa, M.À., et al. (2013) Photosynthesis limitations in three fern species. *Physiol. Plant.* 149: 599–611.

Gallie, D.R. (2013) The role of L-ascorbic acid recycling in responding to environmental stress and in promoting plant growth. *J. Exp. Bot.* 64: 433–443.

Gechev, T.S., Benina, M., Obata, T., Tohge, T., Sujeeth, N., Minkov, I., et al. (2013) Molecular mechanisms of desiccation tolerance in the resurrection glacial relic *Haberlea rhodopensis*. *Cell. Mol. Life Sci.* 70: 689–709.

Geigenberger, P., Thormählen, I., Daloso, D.M. and Fernie, A.R. (2017) The unprecedented versatility of the plant thioredoxin system. *Trends Plant Sci.* 22: 249–262.

Genty, B., Briantais, J.-M. and Baker, N.R. (1989) The relationship between the quantum yield of photosynthetic electron transport and quenching of chlorophyll fluorescence. *Biochim. Biophys. Acta* 990: 87–92.

Hajirezaei, M.R., Peisker, M., Tschiersch, H., Palatnik, J.F., Valle, E.M., Carrillo, N., et al. (2002) Small changes in the activity of chloroplastic $NADP^+$-dependent ferredoxin oxidoreductase lead to impaired plant growth and restrict photosynthetic activity of transgenic tobacco plants. *Plant J.* 29: 281–293.

Harley, P.C., Loreto, F., Di Marco, G. and Sharkey, T.D. (1992) Theoretical considerations when estimating the mesophyll conductance to CO_2 flux by analysis of the response of photosynthesis to CO_2. *Plant Physiol.* 98: 1429–1436.

Hilker, M., Schwachtje, J., Baier, M., Balazadeh, S., Isabel, B., Geiselhardt, S., et al. (2016) Priming and memory of stress responses in organisms lacking a nervous system. *Biol. Rev.* 91: 1118–1133.

Jorge, T.F., Rodrigues, J.A., Caldana, C., Schmidt, R., van Dongen, J.T., Thomas-Oates, J., et al. (2016) Mass spectrometry-based plant metabolomics: metabolite responses to abiotic stress. *Mass Spec. Rev.* 35: 620–649.

König, S., Feussner, K., Kaever, A., Landesfeind, M., Thurow, C., Karlovsky, P., et al. (2014) Soluble phenylpropanoids are involved in the defense

response of Arabidopsis against *Verticillium longisporum*. *New Phytol.* 202: 823–837.

König, J., Muthuramalingam, M. and Dietz, K.J. (2012) Mechanisms and dynamics in the thiol/disulfide redox regulatory network: transmitters, sensors and targets. *Curr. Opin. Plant Biol.* 15: 261–268.

Kopka, J., Schauer, N., Krueger, S., Birkemeyer, C., Usadel, B., Bergmüller, E., et al. (2005) GMD@CSB.DB: the Golm metabolome database. *Bioinformatics* 21: 1635–1638.

Kovinich, N., Kayanja, G., Chanoca, A., Riedl, K., Otegui, M.S. and Grotewold, E. (2014) Not all anthocyanins are born equal: distinct patterns induced by stress in Arabidopsis. *Planta* 240: 931–940.

Laloi, C., Rayapuram, N., Chartier, Y., Grienenberger, J.M., Bonnard, G. and Meyer, Y. (2001) Identification and characterization of a mitochondrial thioredoxin system in plants. *Proc. Natl. Acad. Sci. USA* 98: 14144–14149.

Lázaro, J.J., Jiménez, A., Camejo, D., Iglesias-Baena, I., Martí, M.D.C., Lázaro-Payo, A., et al. (2013) Dissecting the integrative antioxidant and redox systems in plant mitochondria. Effect of stress and S-nitrosylation. *Front. Plant Sci.* 4: 1–20.

Lepistö, A., Pakula, E., Toivola, J., Krieger-Liszkay, A., Vignols, F. and Rintamäki, E. (2013) Deletion of chloroplast NADPH-dependent thioredoxin reductase results in inability to regulate starch synthesis and causes stunted growth under short-day photoperiods. *J. Exp. Bot.* 64: 3843–3854.

Lisec, J., Schauer, N., Kopka, J., Willmitzer, L. and Fernie, A.R. (2006) Gas chromatography mass spectrometry-based metabolite profiling in plants. *Nat. Protoc.* 1: 387–396.

Luedemann, A., Strassburg, K., Erban, A. and Kopka, J. (2008) TagFinder for the quantitative analysis of gas chromatography–mass spectrometry (GC-MS)-based metabolite profiling experiments. *Bioinformatics* 24: 732–737.

Marty, L., Siala, W., Schwarzländer M., Fricker, M.D., Wirtz, M. and Sweetlove, L.J. et al. (2009) The NADPH-dependent thioredoxin system constitutes a functional backup for cytosolic glutathione reductase in Arabidopsis. *Proc.Natl. Acad. Sci. USA* 106: 9109–9114.

Nunes-Nesi, A., Carrari, F., Gibon, Y., Sulpice, R., Lytovchenko, A., Fisahn, J., et al. (2007) Deficiency of mitochondrial fumarase activity in tomato plants impairs photosynthesis via an effect on stomatal function. *Plant J.* 50: 1093–1106.

Mattana, M., Biazzi, E., Consonni, R., Locatelli, F., Vannini, C., Provera, S., et al. (2005) Overexpression of Osmyb4 enhances compatible solute accumulation and increases stress tolerance of *Arabidopsis thaliana*. *Physiol. Plant.* 125: 212–223.

Menezes-Silva, P.E., Sanglard, L.M.P.V., Ávila, R.T., Morais, L.E., Martins, S.C.V., Nobres, P., et al. (2017) Photosynthetic and metabolic acclimation to repeated drought events play key roles in drought tolerance in coffee. *J. Exp. Bot.* 12: 1047–1064.

Mock, H.P. and Dietz, K.J. (2016) Redox proteomics for the assessment of redox-related posttranslational regulation in plants. *Biochim. Biophys. Acta* 1864: 967–973.

Møller, I.M. (2015) Mitochondrial metabolism is regulated by thioredoxin. *Proc. Natl. Acad. Sci. USA* 112: 3180–3181.

Moon, J.C., Lee, S., Shin, S.Y., Chae, H.B., Jung, Y.J., Jung, H.S., et al. (2015) Overexpression of Arabidopsis NADPH-dependent thioredoxin reductase C (AtNTRC) confers freezing and cold shock tolerance to plants. *Biochem. Biophys. Res. Commun.* 463: 1225–1229.

Naranjo, B., Mignée, C., Krieger-Liszkay, A., Hornero-Méndez, D., Gallardo-Guerrero, L., Cejudo, F.J., et al. (2016) The chloroplast NADPH thioredoxin reductase C, NTRC, controls non-photochemical quenching of light energy and photosynthetic electron transport in Arabidopsis. *Plant Cell Environ.* 39: 804–822.

Niinemets, Ü., Cescatti, A., Rodeghiero, M. and Tosens, T. (2005) Leaf internal diffusion conductance limits photosynthesis more strongly in older leaves of Mediterranean evergreen broad-leaved species. *Plant. Cell Environ.* 28: 1552–1566.

Noctor, G., Mhamdi, A. and Foyer, C.H. (2014) The roles of reactive oxygen metabolism in drought: not so cut and dried. *Plant Physiol.* 164: 1636–1648.

Obata, T. and Fernie, A.R. (2012) The use of metabolomics to dissect plant responses to abiotic stresses. *Cell. Mol. Life Sci.* 69: 3225–3243.

Obata, T., Matthes, A., Koszior, S., Lehmann, M., Araújo, W.L., Bock, R., et al. (2011) Alteration of mitochondrial protein complexes in relation to metabolic regulation under short-term oxidative stress in Arabidopsis seedlings. *Phytochemistry* 72: 1081–1091.

Ortiz-Espín, A., Iglesias-Fernández, R., Calderón, A., Carbonero, P., Sevilla, F. and Jiménez, A. (2017) Mitochondrial AtTrxo1 is transcriptionally regulated by AtbZIP9 and AtAZF2 and affects seed germination under saline conditions. *J. Exp. Bot.* 68: 1025–1038.

Piques, M., Schulze, W.X., Höhne, M., Usadel, B., Gibon, Y., Rohwer, J., et al. (2009) Ribosome and transcript copy numbers, polysome occupancy and enzyme dynamics in Arabidopsis. *Mol. Syst. Biol.* 5: 314.

Queval, G. and Noctor, G. (2007) A plate reader method for the measurement of NAD, NADP, glutathione, and ascorbate in tissue extracts: application to redox profiling during Arabidopsis rosette development. *Anal. Biochem.* 363: 58–69.

Reichheld, J.-P., Khafif, M., Riondet, C., Droux, M., Bonnard, G. and Meyer, Y. (2007) Inactivation of thioredoxin reductases reveals a complex interplay between thioredoxin and glutathione pathways in Arabidopsis development. *Plant Cell* 19: 1851–1865.

Reichheld, J.P., Meyer, E., Khafif, M., Bonnard, G. and Meyer, Y. (2005) AtNTRB is the major mitochondrial thioredoxin reductase in *Arabidopsis thaliana*. *FEBS Lett.* 579: 337–342.

Schauer, N., Steinhauser, D., Strelkov, S., Schomburg, D., Allison, G., Moritz, T., et al. (2005) GC-MS libraries for the rapid identification of metabolites in complex biological samples. *FEBS Lett.* 579: 1332–1337.

Schmidtmann, E., König, A.-C., Orwat, A., Leister, D., Hartl, M. and Finkemeier, I. (2014) Redox regulation of Arabidopsis mitochondrial citrate synthase. *Mol. Plant* 7: 156–169.

Serrato, A.J., Pérez-Ruiz, J.M., Spínola, M.C. and Cejudo, F.J. (2004) A novel NADPH thioredoxin reductase, localised in the chloroplast, which deficiency causes hypersensitivity to abiotic stress in *Arabidopsis thaliana*. *J. Biol. Chem.* 279: 43821–43827.

Sienkiewicz-Porzucek, A., Sulpice, R., Osorio, S., Krahnert, I., Leisse, A., Urbanczyk-Wochniak, E., et al. (2010) Mild reductions in mitochondrial NAD-dependent isocitrate dehydrogenase activity result in altered nitrate assimilation and pigmentation but do not impact growth. *Mol. Plant* 3: 156–173.

Sperdouli, I. and Moustakas, M. (2012) Interaction of proline, sugars, and anthocyanins during photosynthetic acclimation of *Arabidopsis thaliana* to drought stress. *J. Plant Physiol.* 169: 577–585.

Spínola, M.C., Pérez-Ruiz, J.M., Pulido, P., Kirchsteiger, K., Guinea, M., González, M., et al. (2008) NTRC new ways of using NADPH in the chloroplast. *Physiol. Plant.* 133: 516–524.

Swann, A.A.L.S., Hoffman, F.M., Koven, C.D. and Randerson, J.T. (2016) Plant responses to increasing CO_2 reduce estimates of climate impacts on drought severity. *Proc. Natl. Acad. Sci. USA* 113: 10019–10024.

Tohge, T. and Fernie, A.R. (2009) Web-based resources for mass-spectrometry-based metabolomics: a user's guide. *Phytochemistry* 70: 450–456.

Tohge, T. and Fernie, A.R. (2010) Combining genetic diversity, informatics and metabolomics to facilitate annotation of plant gene function. *Nat. Protoc.* 5: 1210–1227.

Trewavas, A. (2003) Aspects of plant intelligence. *Ann. Bot.* 92: 1–20.

Urano, K., Maruyama, K., Ogata, Y., Morishita, Y., Takeda, M., Sakurai, N., et al. (2009) Characterization of the ABA-regulated global responses to dehydration in Arabidopsis by metabolomics. *Plant J.* 57: 1065–1078.

Valentini, R., Epron, D., Angelis, P.D.E., Matteucci, G. and Dreyer, E. (1995) In situ estimation of net CO_2 assimilation, photosynthetic electron flow and photorespiration in Turkey oak (*Q. cerris* L.) leaves: diurnal cycles under different levels of water supply. *Plant Cell Environ.* 18: 631–640.

Valliyodan, B. and Nguyen, H.T. (2006) Understanding regulatory networks and engineering for enhanced drought tolerance in plants. *Curr. Opin. Plant Biol.* 9: 189–195.

Virlouvet, L., Ding, Y., Fujii, H., Avramova, Z. and Fromm, M. (2014) ABA signaling is necessary but not sufficient for RD29B transcriptional memory during successive dehydration stresses in *Arabidopsis thaliana*. *Plant J.* 79: 150–161.

Virlouvet, L. and Fromm, M. (2015) Physiological and transcriptional memory in guard cells during repetitive dehydration stress. *New Phytol.* 205: 596–607.

Walter, J., Nagy, L., Hein, R., Rascher, U., Beierkuhnlein, C., Willner, E., et al. (2011) Do plants remember drought? Hints towards a drought-memory in grasses. *Environ. Exp. Bot.* 71: 34–40.

Winger, A.M., Taylor, N.L., Heazlewood, J.L., Day, D.A. and Millar, A.H. (2007) Identification of intra- and intermolecular disulphide bonding in the plant mitochondrial proteome by diagonal gel electrophoresis. *Proteomics* 7: 4158–4170.

Yobi, A., Wone, B.W.M., Xu, W., Alexander, D.C., Guo, L., Ryals, J.A., et al. (2013) Metabolomic profiling in *Selaginella lepidophylla* at various hydration states provides new insights into the mechanistic basis of desiccation tolerance. *Mol. Plant* 6: 369–385.

Yoshida, K. and Hisabori, T. (2014) Mitochondrial isocitrate dehydrogenase is inactivated upon oxidation and reactivated by thioredoxin-dependent reduction in Arabidopsis. *Front. Environ. Sci.* 2: 1–7.

Yoshida, K., Noguchi, K., Motohashi, K. and Hisabori, T. (2013) Systematic exploration of thioredoxin target proteins in plant mitochondria. *Plant Cell Physiol.* 54: 875–892.

Zivcak, M., Brestic, M. and Sytar, O. (2016) Osmotic adjustment and plant adaptation to drought stress. *In* Drought Stress Tolerance in Plants, Vol. 1. Edited by Hossain, M.A. Springer International Publishing, Switzerland.